Mississippi State University
Scholars Junction

Theses and Dissertations | Theses and Dissertations

12-13-2019

Engineering pathological microenvironments for cardiovascular disease studies

Ojaswee Adhikari

Follow this and additional works at: https://scholarsjunction.msstate.edu/td

Recommended Citation
Adhikari, Ojaswee, "Engineering pathological microenvironments for cardiovascular disease studies" (2019). *Theses and Dissertations*. 1884.
https://scholarsjunction.msstate.edu/td/1884

This Graduate Thesis - Open Access is brought to you for free and open access by the Theses and Dissertations at Scholars Junction. It has been accepted for inclusion in Theses and Dissertations by an authorized administrator of Scholars Junction. For more information, please contact scholcomm@msstate.libanswers.com.

www.manaraa.com

Engineering pathological microenvironments for cardiovascular disease studies

By

Ojaswee Adhikari

A Thesis
Submitted to the Faculty of
Mississippi State University
in Partial Fulfillment of the Requirements
for the Degree of Master of Science
in Biomedical Engineering
in the Department of Agricultural and Biological Engineering

Mississippi State, Mississippi

December 2019

www.manaraa.com

Copyright by

Ojaswee Adhikari

2019

www.manaraa.com

Engineering pathological microenvironments for cardiovascular disease studies

By

Ojaswee Adhikari

Approved:

_____

Chartrisa LaShan Simpson
(Major Professor)

_____

Renita E. Horton
(Co-Major Professor)

_____

Steven H. Elder
(Graduate Coordinator)

_____

Keun Seok Seo
(Committee Member)

_____

Jason M. Keith
Dean
Bagley College of Engineering

www.manaraa.com

Name: Ojaswee Adhikari

Date of Degree: December 13, 2019

Institution: Mississippi State University

Major Field: Biomedical Engineering

Major Professor: Chartrisa LaShan Simpson

Title of Study: Engineering pathological microenvironments for cardiovascular disease studies

Pages in Study: 48

Candidate for Degree of Master of Science

Food insecurity is a growing issue in the United States. Iron deficiency is the most common form of nutritional deficiency in patients with endothelial dysfunction and vascular-related diseases. This preliminary study lays the groundwork for the "Nutrient deficiency-on-a-chip" model. Endothelial cells are cultured on mechanically tunable, enzymatically cross-linked gelatin and treated with deferoxamine, an iron chelator, or angiotensin II were used to simulate a nutrient deficient and diseased environment, respectively. As oxidative stress and disturbed barrier function are the most prevailing mechanism of angiotensin II and iron deficiency induced endothelial dysfunction, to test our model we investigated the changes in reactive oxygen species production and VE-cadherin expression in engineered endothelium. Both angiotensin II and deferoxamine treated engineered endothelium showed an increase in oxidative stress and disturbed barrier function. This *in vitro* model can be a useful tool to better understand disease mechanisms associated with nutrient deficiency and identify novel therapeutics.

www.manaraa.com

DEDICATION

I dedicate this research to my parents, Rabi Adhikari and Sagina Adhikari, for their love and support in every step of my academic and professional career.

www.manaraa.com

ACKNOWLEDGMENTS

I would like to acknowledge the faculty and staff at Mississippi State University for their support in my research. First, I would like to acknowledge Dr. Renita E. Horton for her guidance and assistance in this research and throughout my time in graduate school. Second, I would like to thank Dr. LaShan Simpson, Dr. Steven H. Elder, and Dr. Keun Seok Seo for their assistance to this work. I would also like to thank the faculty and staff at I^2AT and Cardiovascular Tissue Engineering Laboratory team for their assistance and support.

www.manaraa.com

TABLE OF CONTENTS

www.manaraa.com

www.manaraa.com

LIST OF FIGURES

www.manaraa.com

CHAPTER I

INTRODUCTION

1.1 Motivation

1.1.1 Food insecurity

Food insecurity is a growing concern in the United States. Food insecurity is a complex problem that impacts people of all communities and all age group. However, people in rural communities, African-Americans especially children, women, and seniors are mostly affected. According to USDA, 11.8% of American household in the US are food insecure where 7.3% of households have low food security and 4.5% of households have very low food security. In Mississippi, approximately, 17.2% of households are considered food insecure [1]. Cardiovascular diseases (CVDs) account for approximately 32% of total death in the world. According to American Heart Association, around 92.1 million US adults have at least 1 type of CVD and by 2030, it is estimated that 43.9% of the US adult population will have some form of CVD [2].

1.1.2 Food insecurity and cardiovascular disease

Studies suggest that poor diets that result from food insecurity can lead to a number of health effects including increased rates of iron-deficiency anemia, acute infection, and cardiovascular diseases. Food insecurity is also associated with clinical evidence of cardiovascular risk factors including hypertension [3]. Similarly, cardiometabolic risk factors including inflammation, endothelial health is influenced by dietary habits [4]. Clearly, maternal food insecurity leads to the birth of babies with low birth weight without catch-up growth, who will in

www.manaraa.com

the long term also have an increased risk of cardiovascular diseases [5]. It is well known that the dietary trace elements containing nutrient supplies like copper, magnesium, iron are highly associated with cardiovascular disease [6]. Various data are available that suggest minimal effects of saturated fat and dietary cholesterol and stronger effects of other compounds such as iron, sodium on cardiovascular effects [7], [8]. Iron deficiency and iron deficiency anemia is the most prevalent nutritional deficiencies in the United States and worldwide. Therefore, food insecure people are significantly more likely to have iron-deficiency anemia than food secure people especially children and women; food insecure children are 2.4 times more likely to have iron deficiency anemia [9], [10]. Despite several studies associating food insecurity, nutritional elements, and cardiovascular disease, cardiovascular disease due to undernutrition is not fully understood.

1.2 Background

1.2.1 Cardiovascular risk factors and endothelial dysfunction

The vascular endothelium is the main point of contact between vessels and blood [11]. The functional integrity of the endothelium is an essential part of vascular homeostasis [12]. Among the various endothelial-derived factors, nitric oxide (NO) plays a crucial role in maintaining vascular homeostasis [13]. Reactive oxygen species (ROS) play a major role in NO-based cell signaling. Oxidative stress affects NO availability in cells and leads to endothelial dysfunction which triggers vascular disorders [12]. Moreover, much evidence has been reported where the amount and duration of cardiovascular risk factor in the patient were independently predicted by the progression of endothelial dysfunction in addition to traditional risk factors [14].

www.manaraa.com

1.2.2 Role of oxidative stress and VE-cadherin in endothelial dysfunction

The progression of endothelial dysfunction is a complex process and is influenced by factors such as oxidative stress and endothelial barrier integrity. Increased oxidative stress weakens the defense mechanism of the vascular endothelium, leading to endothelial dysfunction [15]. Up-regulation of reactive oxygen species (ROS) can lead to the activation of nicotinamide adenine dinucleotide phosphate (NADPH) oxidase, NO inactivation, endothelin expression, and uncoupling of eNOS. During endothelial dysfunction, eNOS acts as a potential ROS generator [16]. Oxidative stress may increase vascular inflammation signaling pathways which increase the superoxide production by inflammatory cells leading to endothelial dysfunction [17].

The endothelium acts as a barrier between surrounding tissue and vessel lumen controlling the passage of blood proteins and cells into the vessel wall. Alteration in junction organization of endothelial cells changes the endothelial reaction with blood proteins and compromise endothelial hemostasis. Vascular Endothelial-cadherin (VE-cadherin), a specific adhesion molecule, located at the junction between the cells is found to have a crucial role in maintaining the barrier function of the endothelium [18]. VE-cadherin is also considered as a major factor in assessing vascular endothelial integrity and permeability.

1.2.3 Role of Angiotensin II (ANG II)

Angiotensin II (ANG II) is a peptide hormone of the renin-angiotensin system. The physiological effects of ANG II are mediated by angiotensin type 1 receptors (AT1Rs), and angiotensin type 2 receptors (AT2Rs) [19]. While ANG II mediates physiological vascular tone cascades and blood pressure regulation, it is also associated with pathological mechanisms such as inflammation, hypertrophy, and endothelial dysfunction. ANG II is considered a potent mediator of oxidative stress [20], [21]. Many ANG II-mediated effects which are implicated in the

www.manaraa.com

pathogenesis of endothelial dysfunction are dependent on ROS [22]–[24]. ANG II up-regulates membrane NAD(P)H oxidases which leads to the generation of ROS, such as superoxide (O_2^-) and hydrogen peroxide (H_2O_2) [25]–[27]. ANG II-mediated generation of superoxide decreases the availability of nitric oxide (NO) in endothelial cells causing endothelial dysfunction [28]–[30]. ANG II can disrupt cell junctions; thus, reducing endothelium integrity [31]. ANG II-treated mice heart tissue cleaved VE-cadherin demonstrating disruption in endothelial barrier [32]. VE-cadherin expression is decreased by ANG II in endothelial cells [33]. Studies suggest that this mechanism is modulated by transforming growth factor (TGF-β1) [34], [35]. TGF- β1 induced disassembly of both adherence and tight junctional complexes and redistribution of cell cytoskeleton in human renal proximal tubular epithelial cells lead to loss of cell-cell contact [36].

1.2.4 Role of deferoxamine (DFO)

Iron deficiency is the most common nutritional deficiency worldwide and is also associated with endothelial dysfunction [37]. Deferoxamine (DFO) is a well-known iron chelating agent and has been used in several studies to induce iron deficiency or to reduce iron overload [38], [39]. Tajima *et al*. demonstrated reduced fat iron concentration and serum ferritin levels in DFO treated mice compared to vehicle treated mice [40]. Increase in oxidative stress has been associated with iron deficiency. Knutson *et al*. reported that severely iron-deficient anemic rats showed a marked increase in lipid peroxidation, suggesting that iron deficiency promotes oxidative stress [41]. Previous morphological and biochemical studies have shown that iron deficiency induced increased oxidative stress is associated with mitochondrial dysfunction [42]. Walter *et al*. reported iron deficiency in Sprague– Dawley rats increased oxidant levels in polymorphonuclear leukocytes (PMNs), and increased mitochondrial DNA (mtDNA) fragmentation [43]; damage to mtDNA correlates with the mitochondrial dysfunction and is

www.manaraa.com

associated with an increase in ROS [44]. Iron deficiency also has a deleterious effect on vascular permeability [45].

1.2.5 Gelatin and microbial transglutaminase (mTG) crosslinked hydrogel as a culture substrate

Traditional *in vitro* systems do not recapitulate extracellular microenvironment [46]. Similarly, due to species-dependent differences, experiments with animal cells and animal models may not be always relevant to humans, which indicates the importance of developing an *in vitro* model with human-derived cells [47]. The extracellular matrix serves as a mechanical support for cells and plays a major role in cellular behavior and expression.

Gelatin is a derivative of collagen, the primary extracellular matrix protein in native heart and endothelium. Therefore, it shows innate structural similarities to the extracellular matrix presenting extensive support for cellular adhesion and proliferation [48]. Gelatin hydrogels are typically not thermostable and form low viscosity solution at physiological temperatures, but it can be chemically crosslinked with enzymes such as microbial transglutaminase (mTG) to convert it into a thermostable hydrogel. Crosslinking with mTG ensures structural integrity with controlled and reproducible gel properties [49]. The gelatin-mTG cross-linked hydrogels have tunable elastic moduli which can be helpful to mimic elastic modulus of heart, improving their robustness and matching native mechanical microenvironment for extended cell culture of engineered cardiac tissue [50]. Due to the greater supply of matrix protein provided by the gelatin substrate, as cells remodel and degrade matrix protein on the surface of the substrate, additional cell adhesion sites throughout the bulk of the gelatin hydrogel become available. Therefore, cardiac tissues remained more viable and contractile in gelatin micro-molded chips over fibronectin microprinted soft PDMS substrates or traditional culture substrates [50].

www.manaraa.com

Similarly, mTG, a purified natural enzyme, has been used in numerous researches to crosslink gelatin and other cell adhesive molecules in order to create more biocompatible, tissue scaffolding or adhesives. *In vivo*, transglutaminase is present in several forms in ECM, blood, and on cell surfaces. They are also expressed in many tissues and have functions in processes such as cell adhesion and migration, posttranslational modification of proteins, extracellular matrix remodeling and fibrin polymerization. In addition, the proteins in the mTG have transamidating activity and catalyze the formation of N-e-(c-glutamyl)lysine protein crosslinks [51]. Chau *et al*. reported transglutaminase treated collagen scaffold enhanced cell attachment and proliferation. It also showed reduced cytotoxicity, increased resistance of scaffold degradation and was resistant to proteolysis [52]. The advantages of using mTG for crosslinked hydrogels clearly indicate their superiority over other conventional crosslinkers ensuring low cytotoxicity and high biocompatibility.

Studies have shown that cells perceive and respond to the rigidity of culture substrate. The substrate stiffness influence cell health and behavior [53]–[55]. Yeung *et.al* studied the effect of substrate stiffness on aorta endothelial cells and demonstrated abrupt changes in shape, cytoskeleton assembly and cell spreading when cultured on surfaces with stiffness ranging from 2 to 55,000 Pa [56]. The extracellular substrate stiffness regulates endothelial cell stiffness via changes in actin cytoskeleton [57]. The mechanical stiffness of the substrate modulates endothelial cells capillary morphogenesis *in vitro* [58]. A significant difference in morphology was observed in cells grown on rigid tissue culture plastic regardless of the presence of ECM proteins as a coating than those grown on the flexible crosslinked gelatin substrates [51]. Similar observations were made when human cardiac microvascular endothelial cells were cultured on gelatin-mTG crosslinked hydrogel substrate. The cells on gelatin mTG hydrogel substrate showed more

www.manaraa.com

elongated cell shape than cells cultured on a regular culture dish (Figure 1.0). This observation complements with the previous study, where endothelial cells grown on softer hydrogel substrate (25 kPa) showed more elongation in shape, whereas those grown on more stiff hydrogel surface (75 kPa) showed more like rounded shape [59]. Substrate stiffness also influences cell adhesion and proliferation [59]. These studies clearly demonstrate the importance of incorporating a softer and flexible culture substrate for *in vitro* experiments. Similarly, in traditional cultures conditions, ECM components are typically either absent or present only as a thin layer of protein adsorbed onto a rigid surface. Moreover, the elastic modulus of healthy human heart ranges from 10-20 kPa approximately [60]. Altering the concentrations of gelatin and mTG will help us to tune the elasticity of culture substrate and recapitulate mechanical properties of native endothelium which is impossible to do with traditional culture plates even coated with ECM. The rigid culture substrates even coated with ECM components do not mimic the mechanical aspects of the *in vivo* microenvironment. Therefore, the traditional *in vitro* culture condition is unable to correlate results to *in vivo* because of the significant differences between the *in vitro* and *in vivo* microenvironments. The gelatin-mTG crosslinked hydrogel based culture substrate may not only provide a more *in vivo*-like-*in vitro* culture environment but will also allow for a wider range of readouts that potentially are more physiologically relevant. This platform will also improve the accessibility of *in vivo* responses of cells to stimuli and could potentially allow for new types of analyses of cellular behavior and function that are impossible to study effectively using traditional culture substrates.

www.manaraa.com

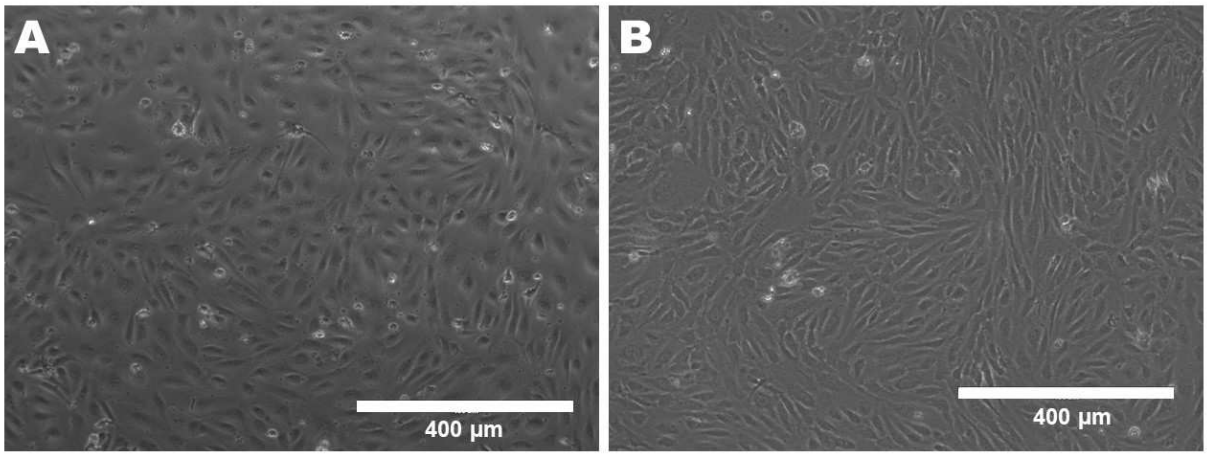

Figure 1.1 A Confluent monolayer of human cardiac microvascular endothelial cells on different culture substrate.

(A) Human cardiac microvascular endothelial cells cultured on a plastic culture substrate. (B). Human cardiac microvascular endothelial cells cultured on a gelatin hydrogel substrate (Scale bars: 400 µm, magnification 10X).

www.manaraa.com

CHAPTER II

DEVELOPMENT OF THE "NUTRIENT DEFICIENCY-ON-A-CHIP" MODEL

2.1 Methods

2.1.1 Materials required

Human cardiac microvascular endothelial cells, Supplement Pack Endothelial Cell GM MV2, Endothelial Basal Medium MV2, Phosphate Buffered Saline (PBS), 0.25% Trypsin-EDTA 1X, Dimethyl sulfoxide, Gelatin, Microbial Transglutaminase (mTG), 184 Silicone Elastomer kit, Bovine serum albumin (BSA), CellRox Green Reagent, anti-VE-cadherin, Triton X-100, Paraformaldehyde, Alexa Fluro^{TM} 546 goat anti-rabbit IgG (H+L), DAPI, Prolong Gold, (3-Aminopropyl)trimethoxy-silane (ATPES), Glutaraldehyde, Ethanol, Angiotensin II (ANG II), Deferoxamine (mesylate) (DFO).

2.1.2 Elastic modulus measurement

2.1.2.1 Atomic force microscopy

The elastic modulus of gelatin-mTG crosslinked chips for different concentrations of gelatin and mTG: 10% gelatin 1% mTG, 10% gelatin 0.8% mTG, 7% gelatin 1% mTG, 7% gelatin 0.8% mTG was measured using Catalyst Atomic Force Microscopy (ZEISS) and conical silicon tip on nitride lever (model: SNL-10 (Veeco); B-f_o = 14-26 KHz). Different concentration of gelatin and mTG solution was mixed together to get the desired concentration and measurement was done. In order to study the changes in elastic modulus of gelatin in culture condition measurement was

www.manaraa.com

also done 24 hours after keeping prepared chips in culture condition. Measurement and analysis were done using Nanoscope 8.15 and Nanoscope Analysis 1.5 software.

2.1.2.2 Mach-1 micromechanical system

The elastic modulus of gelatin-mTG crosslinked hydrogels prepared from two different approaches was measured using the Mach-1 micromechanical system (Biomomentum). The first approach was crosslinking gelatin and mTG solution together to form hydrogel and second was crosslinking pre-cured pure gelatin hydrogel in mTG solution. Mach-1 motion (Model V500c, version 4.3.1.9) software and Mach-1 analysis (version 4.10.17) software were used. Compression test was done to obtain stress and strain values. Young's modulus was calculated using the formula from Hooke's Law:

$$E = \text{stress} / \text{strain} \quad (2.1)$$

$$E = \text{stress} / \text{strain} \quad (2.2)$$

$$E = (F_n / A) / (dl / l_o) \quad (2.3)$$

Where,

E = Young's modulus (N/m^2)

ε = strain

σ = normal stress

F_n = normal force acting perpendicular to the area

A = area

dl = change of length

l_o = initial length

www.manaraa.com

2.1.2.2.1 Crosslinking gelatin and mTG solution together to form a hydrogel

Briefly, 3% agar solution was cured in a petri dish at room temperature and molds were created using a biopsy punch of diameter 8mm. Gelatin and mTG solutions were mixed together to form 7% gelatin 1% mTG mixture and 10% gelatin 1% mTG mixture. The prepared gelatin-mTG solution was introduced to agar molds and cured at room temperature for an hour. After 1 hour, agar was carefully removed to obtain gelatin-mTG crosslinked hydrogel. Prepared gelatin-mTG crosslinked hydrogel cylinders were exposed to UV light for an hour and elastic modulus was measured. Additionally, prepared hydrogel cylinders were incubated in PBS at 37ºC and elastic modulus was measured after 24 hours and 48 hours of incubation.

2.1.2.2.2 Crosslinking pre-cured pure gelatin hydrogel in mTG solution

Agar molds (3%) were prepared as discussed earlier. Sterile gelatin solutions (5% and 7%) were prepared, introduced into the agar molds, and cured at 4ºC overnight. The gelatin hydrogel cylinders were carefully removed from agar mold. Gelatin cylinders were exposed to UV light for an hour and incubated in sterile 1% mTG solution at room temperature for 2 hours. After 2 hours, the mTG solution was aspirated and gelatin-mTG crosslinked hydrogel cylinders were rinsed with PBS. Thus, prepared gelatin-mTG crosslinked hydrogel cylinders were incubated in PBS at 37ºC with continuous swirling using a rocking machine. PBS was changed twice in 24 hours and elastic modulus was measured after 24 hours, 48 hours, and 72 hours of incubation.

www.manaraa.com

2.1.3 Gelatin chip fabrication Process

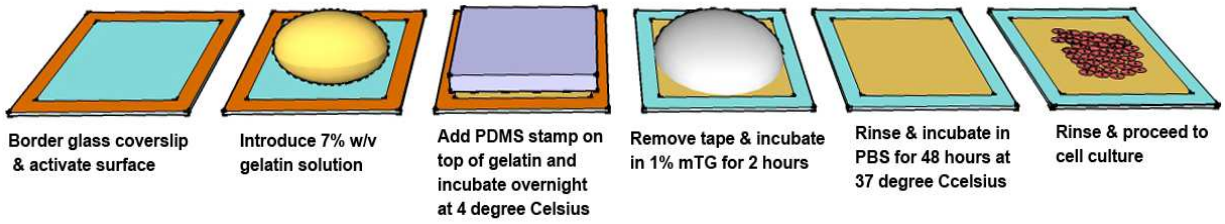

Figure 2.1 Fabrication procedure of crosslinked gelatin hydrogel chip**.**

Glass coverslips (blue) were masked with low-adhesive tape (orange), laser-engraved to expose the center region of glass coverslips, and chemically activated to facilitate gelatin adhesion. 7% gelatin solution (yellow) was introduced on the coverslip and added PDMS stamp (purple) on top of gelatin. After overnight incubation at 4□, the stamp and tape were removed. The construct was then incubated in 1% mTG solution (gray) for 2 hours, rinsed with PBS, incubated in PBS for 48 hours at 37ºC and finally seeded with cells.

Glass coverslips (10mmx10mm) were masked using low-adhesive tape and a laser engraver. Then, the coverslips were chemically activated to facilitate gelatin adhesion. Coverslips were treated with a mixture of Millipore water and 1M NaOH at a 9:1, the ratio for 5 minutes. Again, coverslips were treated with a mixture of 95% ethanol and APTES at a 100:0.5, the ratio for 5 minutes. Coverslips were rinsed with 95% ethanol for 5 minutes three times. After three ethanol rinses, coverslips were treated with a mixture of Millipore water and 70% glutaraldehyde at a 100:0.72 ratio for 30 minutes. Finally, coverslips were rinsed with Millipore water for 5 minutes three times and dried at 65ºC for 15-20 minutes. PDMS stamps were prepared using 184 silicone elastomer kit at a 10:1, base: curing agent, ratio. The solution was then degassed and cured at 65ºC overnight. The stamps were then cut into 10 mm x 10 mm blocks which were used to create a flat gelatin surface. 7% gelatin solution was prepared and dissolved at 55ºC for 20 minutes. To ensure sterility, the gelatin solution was filtered using the 0.2µ filter. The sterile gelatin solution was introduced to an exposed portion of the coverslip and PDMS stamp was added on top of gelatin

www.manaraa.com

solution. The stamped gelatin chip was cured at 4ºC overnight. After curing, PDMS stamp and adhesive tape were carefully removed followed by UV sterilization for an hour. 1% mTG solution was dissolved at room temperature for an hour and was filtered using the 0.2µ filter. The pre-formed gelatin hydrogel layer was crosslinked in mTG solution for 2 hours at room temperature. After 2 hours, the mTG solution was aspirated and the gelatin-mTG crosslinked chip was washed with PBS. Prepared gelatin chip was incubated in PBS at 37ºC for 48 hours before seeding cells to stabilize elastic modulus of the gelatin layer. PBS was changed twice in 24 hours.

2.1.4 Cell culture

Human cardiac microvascular endothelial cells (HCMVEC) were purchased from Lonza and culture was done according to manufacturer's instruction. Cells were cultured in complete EGM-2MV medium supplemented with 5% Fetal Calf Serum (FCS). Passages between 6 and 10 were used for the experiments.

2.1.5 Cell seeding and dosing

HCMVEC were seeded on prepared gelatin-mTG crosslinked chips and dosed with ANG II and DFO in a time-dependent and dose-dependent manner. Cells were dosed with 5 nM, 100 nM ANG II and 50 µM, 200 µM DFO, respectively. Cells were dosed 12 hours after seeding and subsequent doses were in every 24 hours. Drugs were diluted in growth medium supplemented with 5% FCS for dosing up to 24 hours and then with 0.25% BSA was added to growth media supplemented with 0% FCS.

www.manaraa.com

2.1.6 Immunofluorescence study

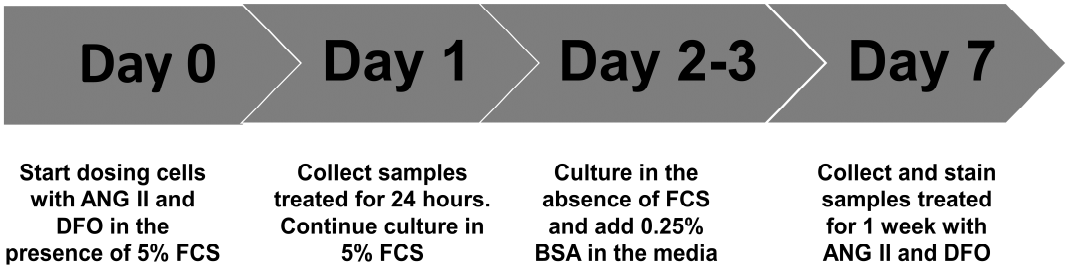

Figure 2.2 Angiotensin II and deferoxamine induced vascular permeability experimental protocol.

Cells were seeded at 30,000 cells /mm^2 and dosed with ANG II (0 nM, 5 nM, and 100 nM) and DFO (0 µM, 50 µM, and 200 µM). Samples were collected 24 hours and 1 week after dosing (Figure 2.2). Briefly, collected samples were fixed and permeabilized using 4% Paraformaldehyde and 0.05% Triton X-100 for 15 minutes. Samples were washed with PBS for 5 minutes 3 times. Cells were incubated with 1% Bovine serum albumin (BSA) to block nonspecific binding, stained with anti-VE-cadherin (primary) (1:200) overnight at 4^{o}C and washed with PBS for 20 minutes three times. Again, cells were stained with secondary antibody Alexa Fluro 546 goat anti-rabbit IgG (H+L) (1:200) and DAPI (0.5:100) for an hour at room temperature and washed with PBS for 20 minutes three times. Samples were mounted using Prolong Gold Anti-fade. Imaging was done in a fluorescence microscope and images were quantified using ImageJ software. The fluorescence intensity of the immunofluorescence stained images was determined using "integrated density" feature in ImageJ under "Analyze-Set Measurements" similar to earlier publications [61]. The

www.manaraa.com

fluorescence intensity was determined using the formula "Corrected total cell fluorescence (CTCF) = Integrated Density - (Area of Section X Background fluorescence)" [62] and expressed in terms of arbitrary units.

2.1.7 Oxidative stress assay

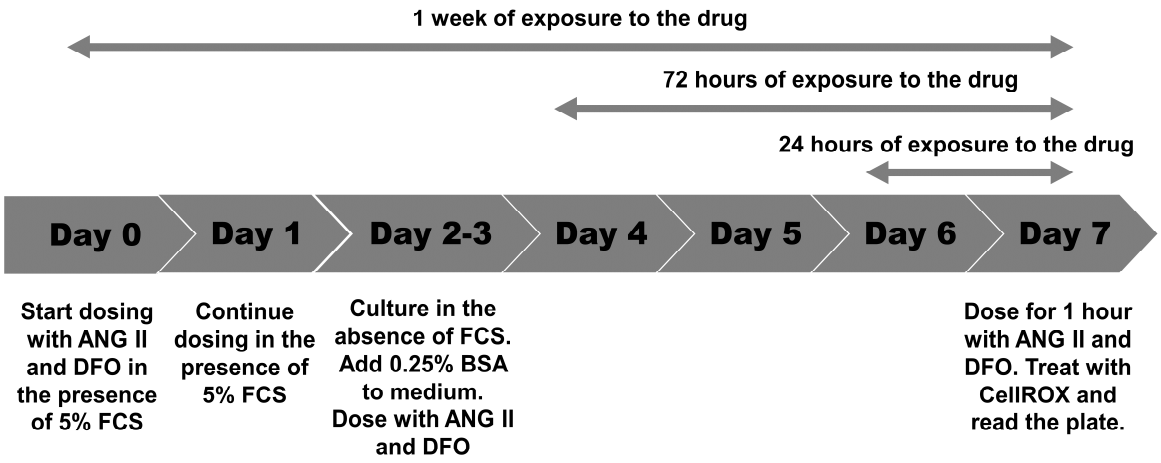

Figure 2.3 Angiotensin II and deferoxamine induced oxidative stress experimental protocol.

Briefly, well-surface of 96-well plate was coated with Gelatin-mTG crosslinked layer following the same procedure for preparing gelatin chips in glass coverslips. Cells were seeded at 50,000 cells per well. Cells were exposed to ANG II (0 nM, 5 nM, 100 nM, and 1 μM) and DFO (0 μM, 50 μM, and 200 μM) for 1 hour, 24 hours, 72 hours and 1 week (Figure 2.3). The kinetics of ANG II and DFO induced production of ROS in the engineered endothelium was assessed using the CellROX Green reagent. CellROX Green reagent is a ROS-sensitive dye and a DNA fluorogenic probe, therefore upon oxidation in an elevated ROS environment, CellROX Green

www.manaraa.com

binds to DNA; thus, its green fluorescence signal is localized primarily in its nucleus and mitochondria [63]–[65]. Cells treated with drugs were treated with CellROX Green Reagent at a final concentration of 5 μM and incubated for 30 minutes at 37°C. After 30 minutes, cells were washed with PBS for 3 times and incubated with growth media. Fluorescence of the oxygenized reagent was measured using a Cytation5 plate reader and Gen 5 3.00 software at 37ºC, 5% CO2. Signal was read every 10 minutes for 2 hours at an excitation and emission wavelength of 485 nm and 528 nm, respectively. Mean fluorescence intensity was used to represent each sample's ROS level. Background signal was determined by running a negative control sample and subtracted from measured signals. Each condition was tested in triplicate.

2.1.8 Statistical analysis

Each experiment is done in three independent experiments (n=3). Data are represented as mean ± standard deviation. For multiple mean comparisons, ANOVA followed by Tukey test was performed with Microsoft Excel. P-values less than 0.05 or 0.01 were considered statistically significant and are also indicated appropriately.

2.2 Results

2.2.1 Elastic Modulus of gelatin-mTG crosslinked chip

The thermal instability of gelatin requires the use of a crosslinker like mTG to stabilize the hydrogel at physiological temperatures. The previous studies have suggested, the elastic modulus of gelatin and mTG crosslinked hydrogel increases with the increase in concentration and crosslinking time of gelatin and mTG. Studies show that the cell culture substrate stiffness can influence cellular behavior [55], [66]. Therefore, one of the goals was to create a stable elastic modulus for the culture substrate. We examined 7% and 10% gelatin formulations with atomic

www.manaraa.com

force microscopy (AFM). The mTG concentration (0.8% and 1%) was also varied to determine the optimal concentration that would result in an acceptable modulus yet durable enough to withstand handling required for chip assembly. An equal volume of gelatin and mTG solutions were mixed together to get the desired concentration. All formulation tested resulted in gels that were within the range 10-20 kPa (Figure 2.4A). We found that the modulus of gelatin-mTG crosslinked hydrogel increased with time suggesting a potential dynamic stiffening within the gels. Therefore, our next question was would the elastic modulus of crosslinked gelatin be stable when kept in culture condition. We incubated the prepared chips in culture condition (in PBS at 37^{o}C 5% CO_2) for 24 hours and measured changes in elastic modulus. We observed the elastic modulus of 10% gelatin 1% mTG significantly increased from 20.60 ± 3.29 kPa to 76.72 ± 20.34 kPa (Figure 2.4A, 2.4B) in 24 hours. Similarly, the elastic modulus of 7% gelatin 1% mTG significantly increased from 13.92 ± 1.88 kPa to 38.45 ± 5.35 kPa (Figure 2.4A, 2.4B) in 24 hours. Therefore, the elastic modulus of gelatin-mTG crosslinked hydrogel significantly increased with increase in concentration and time (Figure 2.4A, 2.4B). We conducted a similar study using Mach-1 to compare the results from AFM and observed similar results. Both 7% gelatin 1% mTG (Figure 2.5A) and 10% gelatin 1% mTG (Figure 2.5B) showed a significant increase in elastic modulus in 24 hours and 48 hours when incubated in culture condition.

www.manaraa.com

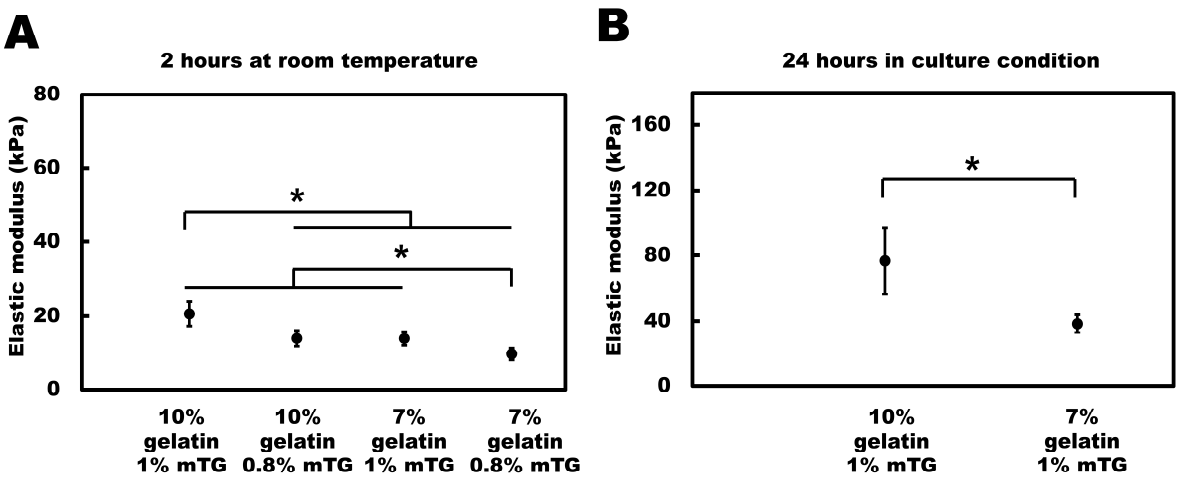

Figure 2.4 The elastic modulus for different concentrations of gelatin and microbial transglutaminase measured with atomic force microscopy.

(A) Displays elastic modulus for different concentrations of gelatin and mTG after 2 hours of crosslinking. (B) Displays elastic modulus for different concentrations of gelatin and mTG crosslinked hydrogel after incubating for 24 hours in culture condition (in PBS at 37°C, 5% CO_2, and a humidified atmosphere) (n = 3, Mean ± Standard deviation, * indicates P-value < 0.01)

www.manaraa.com

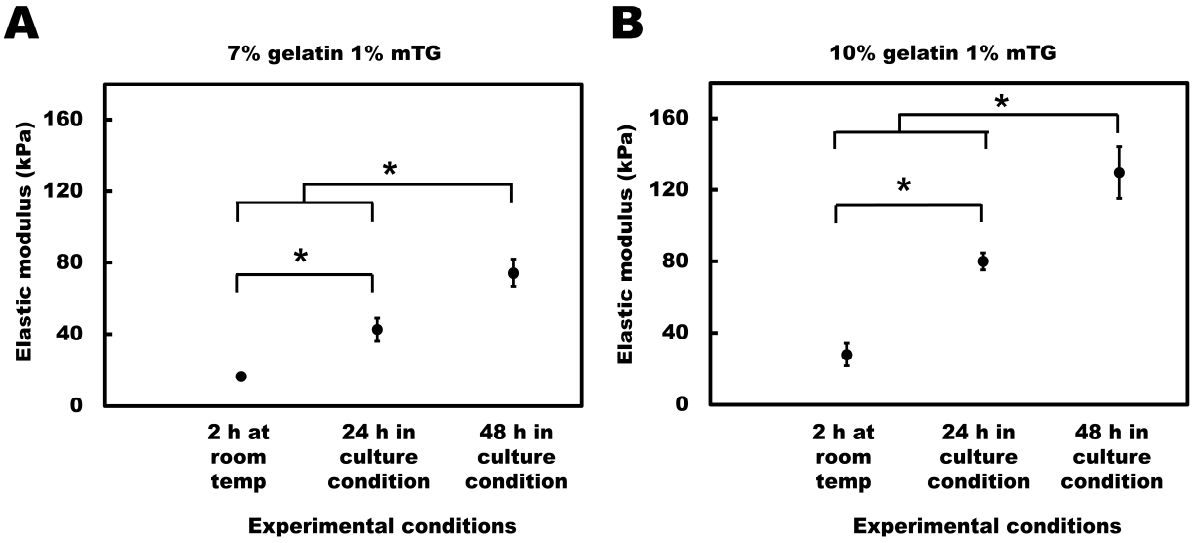

Figure 2.5 The elastic modulus for different concentrations of gelatin-microbial transglutaminase crosslinked hydrogel measured with Mach-1.

Gelatin and mTG solutions were mixed together to get the desired concentration. (A) Displays elastic modulus for 7% gelatin and 1% microbial transglutaminase. (B) Displays elastic modulus for 10% gelatin and 1% microbial transglutaminase. Crosslinked hydrogels were incubated in culture condition (in PBS at 37°C, 5% CO_2, and a humidified atmosphere) for 24 hours and 48 hours without a rocker. (n=3, Mean ± Standard deviation, * indicates P-value < 0.01)

Previous results of elastic modulus obtained from Mach-1 showed a significant increase in elastic modulus of gelatin and mTG crosslinked hydrogel when kept in a culture condition. Therefore, we tried another approach of chip fabrication where pre-cured gelatin hydrogel was incubated in mTG solution and then was swirled continuously in PBS. We measured temporal changes in elastic modulus over 72 hours to determine the time needed for crosslinking stabilization. There was no significant increase in elastic modulus for both 5% gelatin hydrogel crosslinked in 1% mTG solution (Figure 2.6A) and 7% gelatin hydrogel crosslinked in 1% mTG solution (Figure 2.6B) when incubated in culture condition for 72 hours using a rocker. Although,

www.manaraa.com

the elastic modulus of 5% gelatin hydrogel crosslinked in 1% mTG solution was more stable and closely matched the elastic modulus of native heart (10-20 kPa) in comparison to 7% gelatin hydrogel crosslinked in 1% mTG solution, the gels often fractured during later fabrication steps and handling, limiting their utility as a robust experimental platform. Thus, for further study, we chose to continue with 7% gelatin hydrogel cross-linked in 1% mTG solution, which had an elastic modulus of approximately 17 kPa and better matched the elastic modulus of the native heart compared to traditional culture substrates. Moreover, the thickness of the gelatin layer on the prepared chip was dictated by the thickness of the adhesive tape which is approximately 100μm. Therefore, the thickness of gelatin hydrogel should be sufficiently thick to minimize the effects of an underlying rigid glass coverslip.

www.manaraa.com

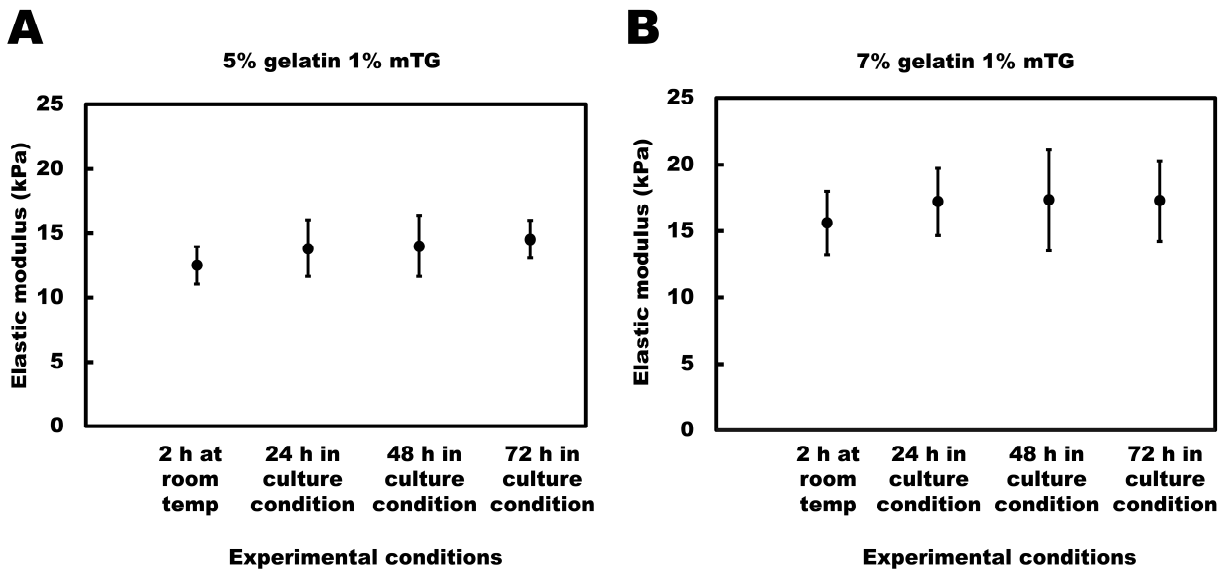

Figure 2.6 The elastic modulus for different concentrations of pre-cured gelatin hydrogels crosslinked in microbial transglutaminase solution and measured on Mach-1.

(A) 5% gelatin and (B) 7% gelatin solution were cured for overnight at 4ºC in agar mold followed by UV sterilization for an hour. Pre-cured hydrogels were incubated in 1% microbial transglutaminase solution for 2 hours at room temperature. Crosslinked hydrogels were also incubated in culture condition (in PBS at 37°C, 5% CO_2, and a humidified atmosphere) for 24 hours and 48 hours and 72 hours with a rocker. (n=3, Mean ± Standard deviation).

www.manaraa.com

2.2.2 Angiotensin II-induced oxidative stress

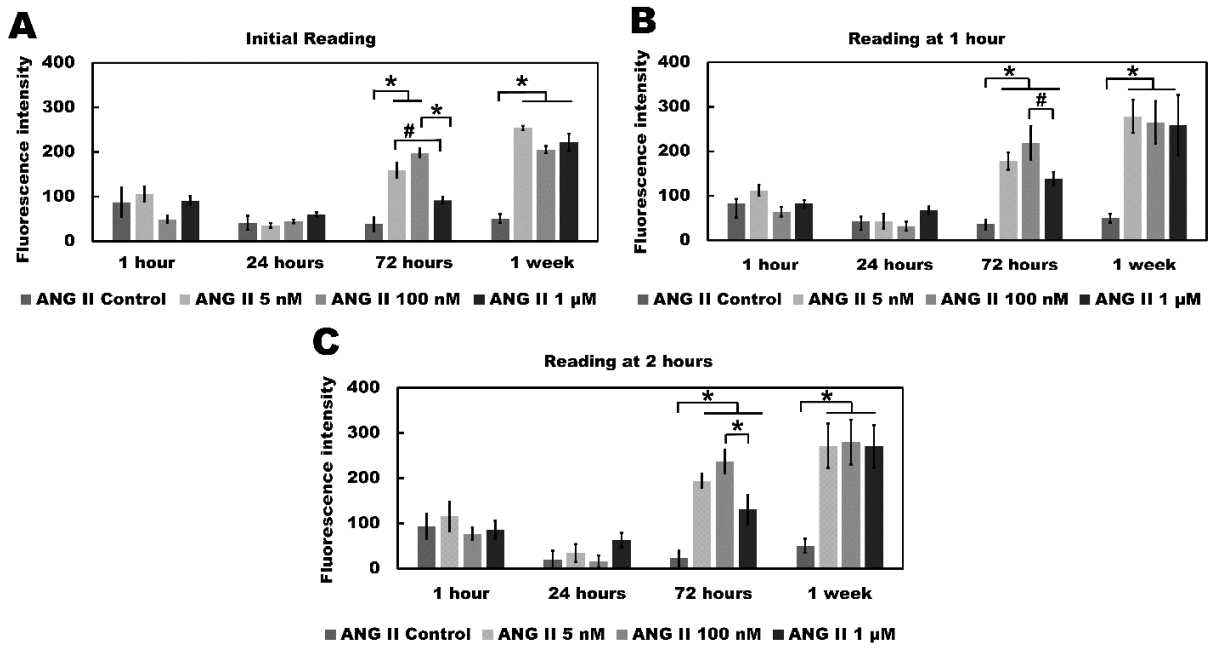

Figure 2.7 Angiotensin II-induced oxidative stress.

HCMVEC were treated with 0, 5 nM, 100 nM, and 1 µM ANG II for 1 hour, 24 hours, 72 hours and 1 week. ROS production was evaluated using CellROX Green reagent. (A) The graph represents ROS production at initial plate reading. (B) The graph represents ROS production at 1 hour of plate reading. (C) The graph represents ROS production at 2 hours of plate reading. There was no significant difference in ROS production at 1 hour and 24 hours ANG II-treated cells, however, at 1 week and 72 hours ANG II-treated cells produced significantly higher ROS than control cells. (n=3, Mean ± Standard deviation, * indicates P-value < 0.01 relative to respective time point and # indicates P-value < 0.05 relative to respective time point).

HCMVEC was treated with 0, 5 nM, 100 nM and 1 µM ANG II for 1 hour, 24 hours, 72 hours and 1 week. The kinetics of ANG II-induced production of ROS in HCMVEC was studied for 2 hours in an interval of every 10 minutes. During the initial reading (Figure 2.7A), we observed that there was no significant difference in ROS production between control, 5 nM, 100 nM, and 1 µM ANG II-treated cells for 1 hour and 24 hours. The 72 hours and 1 week time-point 5 nM, 100

www.manaraa.com

nM and 1 μM ANG II produced higher ROS than control. At 72 hours, 100 nM and 5 nM ANG II treatment produced significantly higher ROS than control and 1 μM ANG II treatment. At 1week, 5 nM, 100 nM, and 1 μM produced significantly higher ROS than control. However, there was no significant difference among the ANG II-treated groups with 1 week of exposure.

Similar results were observed in 1 hour and 2 hours of plate reading (Figure 2.7B, 2.7C). There was no significant change in ROS production in cells after 1 hour and 2 hours of reading. Similar to initial reading, at 1 hour and 2 hours of reading time point, there was no significant difference in ROS production between control, 5 nM, 100 nM, and 1 μM ANG II treatment for 1 hour and 24 hours. Cells treated for 72 hours and 1 week showed significantly higher oxidative stress in 5 nM, 100 nM, and 1 μM than in control. The only difference observed was that during initial reading, 72 hours 5 nM ANG II treatment produced significantly higher ROS than 1 μM ANG II, however, during 1 hour and 2 hours reading we observed no significant difference in ROS production between 5 nM and 1 μM ANG II treatment for 72 hours.

Similarly, during the kinetic study of ANG II-induced ROS production for 2 hours we did not observe any significant change in kinetic ROS production by control, 5 nM, 100 nM and 1 μM ANG II-treated for 1 hour, 24 hours, 72 hours and 1 week, however, at 72 hours 1 μM ANG II-treated cells produced higher ROS throughout the 2 hours of kinetic experiment (Figure A.1).

www.manaraa.com

2.2.3 Deferoxamine induced oxidative stress

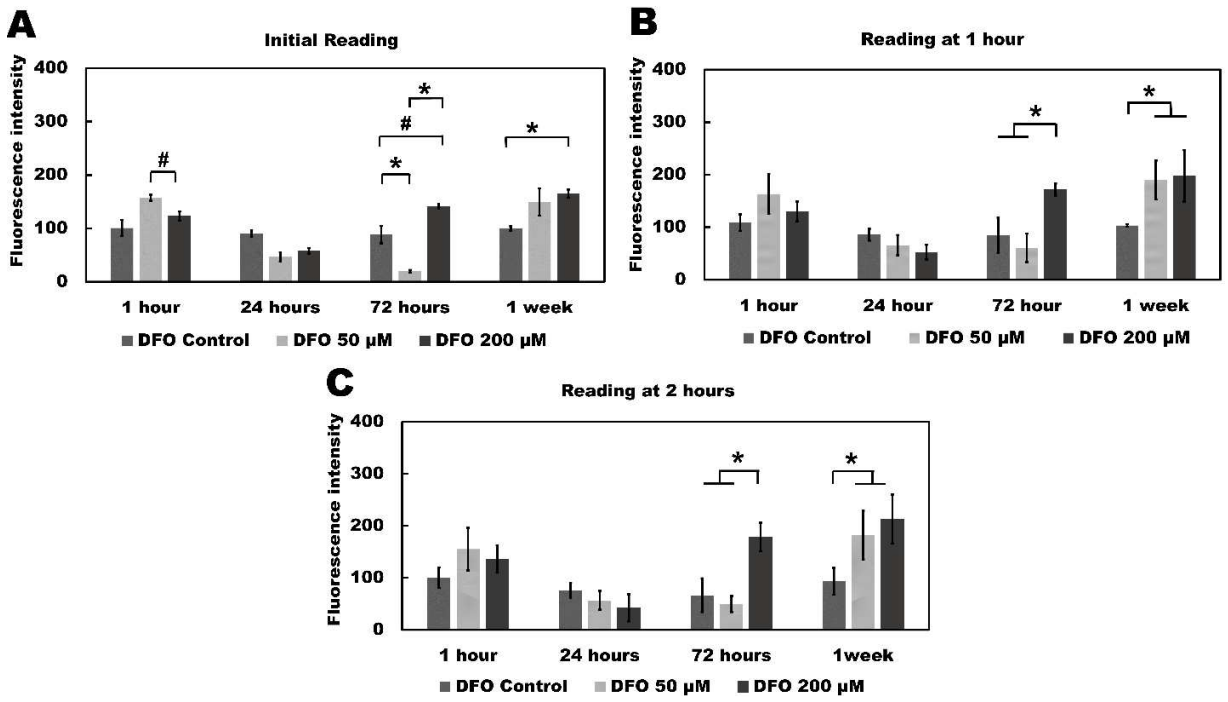

Figure 2.8 Deferoxamine induced oxidative stress.

HCMVEC were treated with 0, 50 µM and 200 µM DFO for 1 hour, 24 hours, 72 hours and 1 week. ROS production was evaluated using CellROX Green reagent. (A) The graph represents ROS production at initial plate reading. (B) The graph represents ROS production at 1 hour of plate reading. (C) The graph represents ROS production at 2 hours of plate reading. There was no significant difference in ROS production at 1 hour and 24 hours DFO treated cells, however, at 1 week and 72 hours a significant difference in ROS production was observed between DFO treated and control cells. (n=3, Mean ± Standard deviation, * indicates P-value < 0.01 relative to respective time point and # indicates P-value < 0.05 relative to respective time point)

HCMVEC was treated with 0, 50 µM and 200 µM DFO for 1 hour, 24 hours, 72 hours and 1week. The kinetics of DFO induced ROS production in HCMVEC was studied for 2 hours in an interval of every 10 minutes. The initial reading (Figure 2.8A) revealed that at 1 hour 50 µM DFO treated cells produced higher ROS than 200 µM DFO and control. At 24 hours there was no significant difference between control, 50 µM and 200 µM DFO treated cells. However, at 72

www.manaraa.com

hours 200 µM DFO produced significantly higher ROS than 50 µM DFO and control cells. At 1 week time point, 200 µM and 50 µM DFO produced higher oxidative stress than control. However, there was no significant difference among the DFO treated groups with 1week of exposure.

Similar results were observed in 1 hour and 2 hours of reading (Figure 2.8B, 2.8C). Similar to initial reading, at 1 hour and 2 hours of reading time point, cells treated with 50 µM DFO for 1 hour showed slightly higher oxidative stress than 200 µM and control. There was no significant difference between control, 50 µM and 200 µM DFO treated cells for 24 hours. At 72 hours, 200 µM DFO produced significantly higher oxidative stress than 50 µM DFO and control treated cells. At 1 week, 200 µM and 50 µM DFO produced significantly higher oxidative stress than control. During the initial reading, 1 week 50 µM DFO exposed and control cells did not show a significant difference in ROS production. However, at 1 hour and 2 hours plate reading 1week 50 µM DFO treatment produced significantly higher ROS than control (Figure 2.8). Similarly, there was no significant change in ROS production during the kinetic experiment for cells treated with 1 hour DFO. Insignificant fluctuations in the kinetic ROS production were observed for 24 hours of DFO exposure. Cells treated with 50 µM DFO for 72 hours significantly increased ROS production and reached a peak at approximately 50 minutes and began to decrease after 50 minutes. Only 50 µM DFO treated for 24 hours and 72 hours showed a significant change in kinetic ROS production (Figure A.2).

2.2.4 Effects of angiotensin II on barrier function

The engineered endothelium were treated with 5 nM, and 100 nM of ANG II for 24 hours and 1 week and were stained with anti-VE-cadherin. ANGII-induced endothelial barrier dysfunction was studied and compared against untreated controls. A discontinuous and disrupted

www.manaraa.com

VE-cadherin staining pattern was observed in cells treated with 5 nM and 100 nM ANG II for 1 week (Figure 2.9). The fluorescence signal along the cell junctions of cells exposed to 5 nM and 100 nM ANG II-for 1week was significantly low than untreated cells (Figure 2.9, 2.10). Further, the staining pattern and intensity did not change in cells treated with ANG II for 24 hours (Figure 2.9, 2.10).

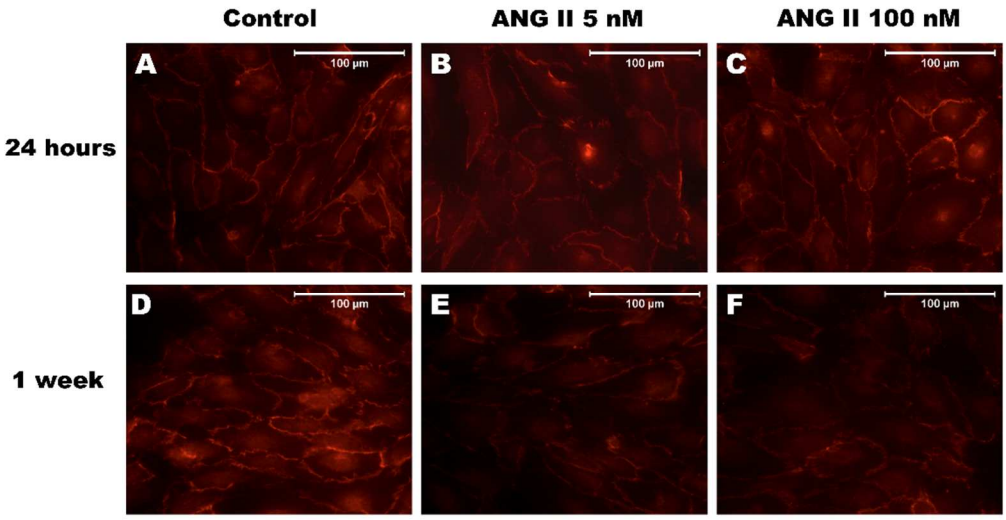

Figure 2.9 Effect of angiotensin II on barrier function.

Engineered endothelium were treated with ANG II (0, 5 nM, and 100 nM) for 24 hours and 1 week. Collected samples were stained with VE-cadherin to study barrier function. The fluorescence intensity and staining pattern remained the same for (A) Control 24 hours (B) 5 nM ANG II 24 hours (C) 100 nM ANG II 24 hours and (D) Control 1 week, however, reduced fluorescence intensity and disrupted staining pattern was observed on cells treated with (E) 50 nM ANG II 1 week and (F) 100 nM ANG II 1 week. (Scale bars: 100 µm, magnification of 40X, n=3)

www.manaraa.com

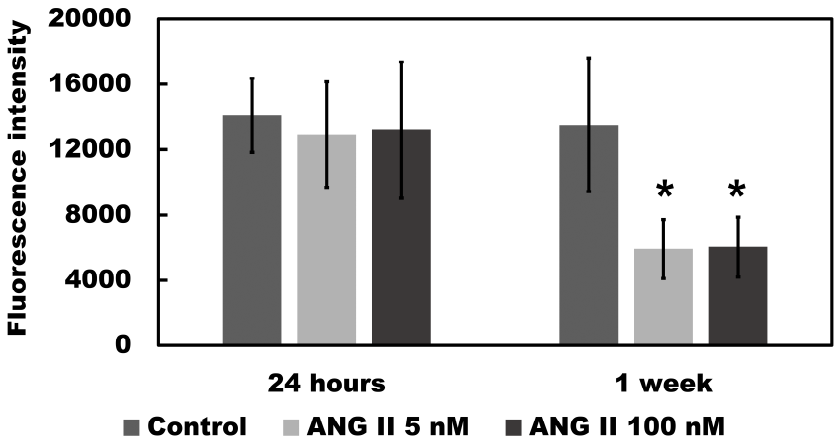

Figure 2.10 Effect of angiotensin II on VE-cadherin.

Engineered endothelium were treated with ANG II (0, 5 nM, and 100 nM) for 24 hours and 1 week. Collected samples were stained with VE-cadherin to study barrier function. There was no significant difference between ANG II-treated and control cells at 24 hours, however, at 1 week significantly reduced fluorescence intensity was observed on cells treated with 5 nM and 100 nM ANG II. (n=3, Mean ± Standard deviation, * indicates P-value < 0.01 vs control of respective time point)

2.2.5 Effects of deferoxamine on barrier function

To investigate DFO induced endothelial barrier dysfunction, the engineered endothelium were treated with 0, 50 μM, and 200 μM DFO for 24 hours and 1 week. The treated engineered endothelium were stained with anti-VE-cadherin and were observed under a fluorescence microscope. A fragmented and discontinuous staining pattern was observed in cells treated with DFO for both 24 hours and 1 week (Figure 2.11). The fluorescence intensity of VE-cadherin was significantly lower than control after 24 hours or 1 week of treatment with 50 μM and 200 μM DFO (Figure 2.11, 2.12).

www.manaraa.com

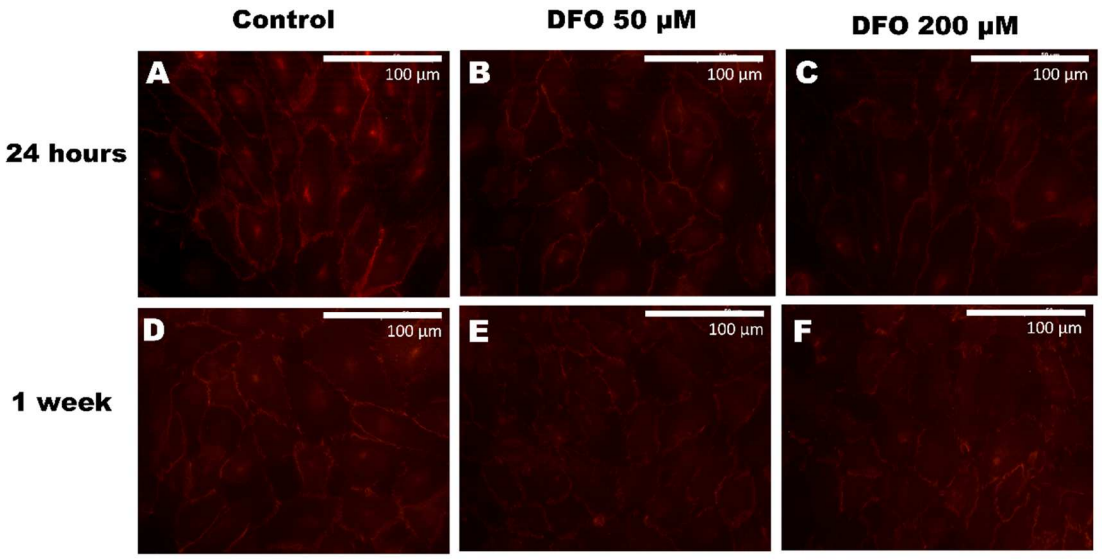

Figure 2.11 Effect of deferoxamine on barrier function.

Engineered endothelium were treated with DFO (0 µM, 50 µM, and 200 µM) for 24 hours and 1 week. Collected samples were stained with VE-cadherin to study barrier function. Reduced fluorescence intensity and a disrupted VE-cadherin pattern were observed on cells treated with 50 µM and 200 µM DFO for 24 hours and 1 week (B, C, E, and F). (Scale bars: 100 µm, magnification of 40X, n=3)

www.manaraa.com

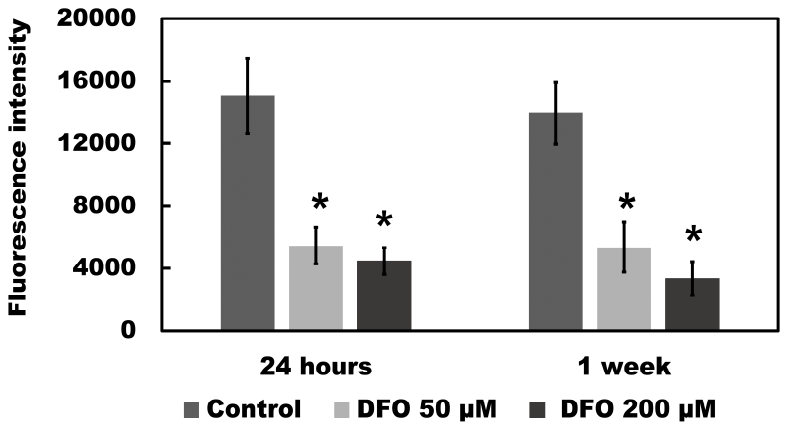

Figure 2.12 Effect of deferoxamine on VE-cadherin.

Engineered endothelium were treated with DFO (0, 50 µM and 200 µM) for 24 hours and 1 week. Collected samples were stained with VE-cadherin to study barrier function. Significantly reduced fluorescence intensity was observed on cells treated with 50 µM and 200 µM DFO for 24 hours and 1 week. (n=3, Mean ± Standard deviation, * indicates P-value < 0.01 vs control of respective time point)

2.3 Discussion

In this study, we created a gelatin-based *in vitro* system which is the preliminary stages of the "nutrient-deficiency on a chip" model. We first created an engineered endothelium by culturing HCMVEC on the crosslinked gelatin hydrogel chip, then we treated the engineered endothelium with DFO (0, 50 µM, and 200 µM) to induce iron deficiency. As previous studies suggest ANG II has been shown to induced endothelial dysfunction and also contributes to the pathophysiology of cardiovascular diseases, we also treated engineered endothelium with ANG II (0, 5 nM, 100 nM, and 1 µM). We tested our model by studying oxidative stress and the barrier function of the engineered endothelium.

www.manaraa.com

ANG II is strongly incriminated in the pathogenesis of vascular injury and therefore is a growing body of evidence that ANG II induces oxidative stress in cells [26], [67]–[69]. In this study, we observed a significant rise in ROS production in cells treated with 5 nM, 100 nM, and 1 μM ANG II for 72 hours and 1week was observed in comparison to control cells, which suggests that exposure to ANG II elevates the oxidative stress in cells. Our data complement that exposure of endothelial cells to ANG II induces oxidative stress *in vitro* and *in vivo* [67]. Generation of ROS by ANG II may contribute to progressive vascular injury through diverse mechanisms. Oxidative stress in smooth muscle cells and endothelial cells may arise from stimulation of membrane-bound NADH/NADPH oxidase which increases the generation of superoxide anion [26], [69]. Besides endothelial cells, NADH/NADPH oxidase-induced oxidative effects of ANG II has also been found in smooth muscle cells, mesangial cells and LLC-PK1 cells in vitro [70], [71]. Also, administration of ANG II has been found to elevate several markers of oxidative injury such as lipid peroxidation, protein carboxyl content, hydroxyl radicals (OH) [67]. Besides, activation of NADPH/NADH oxidase system ANG II also exerts oxidation stress via stimulation of numbers of cytokines which are pro-oxidants [72], [113].

Iron is an important trace element for fundamental metabolic processes in living cells. Both, iron overload and iron deficiency are associated with the production of ROS that includes superoxide radical anion, hydrogen peroxide, and the hydroxyl radical [73]. In this study, we observed a significant rise in ROS production in cells treated with DFO for 72 hours and 1week in comparison to control cells. The results suggested that DFO induced iron deficiency elevated the oxidative stress in cells. Also, exposure to 50 μM DFO for 24 hours and 72 hours showed a significant change in kinetic ROS production. Iron deficiency derived oxygen stress can cause organ dysfunction via damage to DNA, lipids, and proteins [74]. Jagadeesen *et al*. studied lipid

www.manaraa.com

peroxidation and activities of different antioxidant enzymes in iron deficiency and found iron-deficient rats showed an elevation in lipid peroxidation and were more susceptible to oxidative stress. The increase of superoxide radical is fostered by iron inadequacy, leading to persistence of O_2 radicals which give rise to other ROS such as OH [75]. Walter *et al*. reported iron-deficient rats developed free radical mitochondrial DNA (mtDNA) damage [43]. Impaired mtDNA induces an increase in ROS production [76]. Latif *et al*. reported that iron-starved cells demonstrated a 10-fold increase of ROS levels and increased lipid peroxidation compared to cells grown with normal iron [77].

Oxidants create cytotoxicity to cells in the vascular system. Oxidants also induce activation of endothelial cells. ROS upregulates pro-inflammatory and chemotactic substances, and also promotes inflammatory responses [78], [79], [112]. Additionally, there is mounting evidence that oxidative stress induces factors which up-regulates pro-inflammatory species like transcription factor, namely, nuclear factor-kβ (NF- kβ); pro-inflammatory and chemotactic substances adhesion molecules, selectin (E-selectin and P-selectin), T-cell chemoattractants (RANTES), and the monocyte-chemo attractants (MCP-1) [78], [79], [112]. Previous studies suggest that ANG II promotes these factors [72], [80]–[82]. Therefore, the elevation of ROS by ANG II and DFO in engineered endothelium contributes to the progression of factors that causes endothelial dysfunction and vascular injury.

Similarly, we observed no significant difference in VE-cadherin intensity in cells treated with ANG II for 24 hours, however, a fragmented pattern and lower fluorescence signal of VE-cadherin was observed in 1week ANG II treatment. Our results regarding the endothelial barrier function are consistent with several published observations. Yoshioka *et al*. also demonstrated ANG II treatment caused disruption of VE-cadherin in endothelial cell junctions resulting in

www.manaraa.com

defective junction assembly [83]. Pupilli *et al*. evaluated the role of ANG II in regulating vascular endothelial growth factor (VEGF)- a prominent regulator for vascular permeability in human mesangial cells *in vitro* and found that both mRNA and secretion of VEGF was significantly higher in cells treated with 10 nM, 100 nM, and 1 μM ANG II than control [84]. Similarly, Sano *et al*. studied the relationship between ANG II, VEGF and vascular permeability in human microvascular endothelial cells. VEGF induced disruption of VE-cadherin was suppressed by ANG II type 1 receptor (AT1R) blocker *in vitro*. AT1R-deficient mice also inhibited hyperpermeability and VEGF-induced gap formation between endothelial cells [85]. We also observed that DFO treatment induced discontinuous and fragmented VE-cadherin with lower intensity in 24 hours and 1 week. Beerepoot *et al*. found that iron deficiency induced by several iron chelators including DFO up-regulated vascular endothelial growth factor (VEGF), which is a most potent vascular permeability factor [38]. VEGF treatment causes disruption in intercellular junctions of capillaries and small venules within minutes of treatment [86]. Several other studies describe the mechanisms of VEGF induced vascular permeability [87]–[89]. These findings strongly suggest ANG II and iron deficiency affects endothelial barrier function. The observed result of ANG II or DFO induced decrease of adherens junction protein VE-cadherin is due to the association of ANG II or iron deficiency on cell junction. Previous studies suggest oxidative stress is directly responsible for endothelial cell leakiness [90], [91]. Therefore, the ANG II and DFO induced disruption in VE-cadherin may be promoted by ANG II and DFO induced oxidative stress. ROS produced by endothelial cells at reoxygenation increases the formation of gap structures between endothelial cells via changes in actin cytoskeletal dynamics. P. L. Apopa *et al*. demonstrated that elevation of intracellular ROS causes disruption of VE-cadherin and increases permeability in a confluent monolayer of human microvascular endothelial cells through

www.manaraa.com

cytoskeletal damage [91]. T. N. Meyer *et al*. developed a model in which oxidative stress compromises cell junction. Exposure to hydrogen peroxide for 30 minutes or 60 minutes significantly decreased transendothelial resistance and observed disruption in junction proteins cadherin, ZO-1, occludin during immunofluorescence study [92]. Previous studies also suggest that exposure of endothelial cell monolayers to ROS generators like glucose/glucose oxidase or xanthine/xanthine oxidase increases endothelial cell permeability in a dose-dependent manner through oxidative stress [93], [113].

Several studies suggest the role of ANG II in the redistribution of the cytoskeletal system [94]–[96]. Similarly, iron is critical for normal functioning of the signaling cascade that regulates cytoskeletal dynamics [97]–[99]. Numerous studies also refer to coordination between cytoskeletal system, endothelial cell adhesion and barrier function. The cadherins and cytoskeletal system bind via catenins (α-, β-, and γ-catenins). Therefore, remodeling of the cytoskeletal system affects the regulation of cadherins [100], [101]. Therefore, ANG II and DFO induced inhibition of VE-cadherin may be due to ANG II and DFO-induced oxidative stress itself and cytoskeletal remodeling induced by ANG II and DFO.

We assert that the developed model of which is a preliminary step towards nutrient-deficiency-on-a-chip can serve as a suitable platform for investigating nutrient deficiency disease mechanism and pharmaceutical applications. In this study, we created a DFO induced nutrient deficient endothelium model and ANG II-induced endothelial dysfunction model. The DFO induced iron deficient model mimics features of endothelium dysfunction and offers an ability to independently study the nutrient deficient effects on the function of the endothelium. The present study highlights engineered endothelium that are cultured in the static condition, however, the vascular endothelium is in intimate contact with blood and is directly exposed to various fluid mechanical

www.manaraa.com

forces generated by pulsatile blood flow. The hemodynamic force has a crucial role in regulating endothelial structure and function [102]. The functional phenotype of vascular endothelium is dynamically responsive to the biomechanical stimuli generated by pulsatile flow of blood. The *in vitro* flow systems help to investigate the fluid shear stress stimulated cell biological effects in cultured monolayer of endothelium. The *in vitro* flow studies are able to recapitulate the features of endothelial cells that are similar to endothelial cells *in vivo* [103]. Vascular endothelial cells change cell shape from polygonal to ellipsoidal and become uniformly oriented with the flow when subjected to time and force dependent fluid shear stress [114]. Blood flow induced wall shear stress also lead to dynamic changes in intracellular Ca^{2+} concentrations which is essential for generation of ROS and activation of signaling pathways that result in disassembly of VE-cadherin and trigger endothelial permeability [104]–[106]. It has also been suggested that changes in shear stress cause reorganization of junction-associated proteins which affect permeability in endothelial cells [107]. Endothelial cells cultured under static conditions show low bio-ability of NO production, as well as the synthesis of eNOS mRNA and protein in comparison to cell subjected to shear stress [108], [109]. Developing a gelatin hydrogel based microfluidic device with similar gelatin culture substrate fabricating technology in future can be useful to overcome the limitation of this study and investigate endothelial cells under flow conditions which will more closely mimic the native endothelium system.

www.manaraa.com

2.4 Conclusions and future work

2.4.1 Conclusions

In the present study, we probed to recapitulate DFO induced nutrient deficiency model using an engineered endothelium. We demonstrated that ANG II and DFO-induced iron deficiency increases the oxidative stress in a dose-dependent and time-dependent manner. ANG II and DFO induced iron deficiency also disrupts the barrier function in HCMVEC and increases vascular permeability. Increased oxidative stress and disturbed barrier function contribute to endothelial dysfunction triggering cardiovascular events. The developed model can be further utilized to investigate genetic, morphological, and functional changes due to iron deficient diet on the model endothelium. This biomimetic nutrient deficient endothelium platform can be beneficial to investigate the underlying mechanisms of endothelial dysfunction in cardiovascular disease.

2.4.2 Future work

Gelatin-based microfluidic technologies are emerging as a promising tool for various applications in tissue engineering and cell biology, such as co-culture, microvasculature, and tissue assembly [51] [110]. In this study, we highlighted the nutrient deficient model which consists of endothelial cells however, the cardiovascular system consists of cells such as smooth muscle cells, fibroblasts. Therefore, a co-culture system can be developed in the future using a similar chip fabrication technique to understand the relation between nutrient deficiency and CVD. The fabrication technique developed in this research can also be helpful to develop a gelatin hydrogel based biomimetic vasculature chip containing simplified branching geometries that mimic the mechanical and structural properties of the native vasculature. Similarly, in this study, we probed oxidative stress and endothelial barrier function on the DFO induced nutrient deficient model and

www.manaraa.com

ANG II-induced endothelial dysfunction model. However, endothelial dysfunction includes several other markers such as nitric oxide generation, adhesion molecules, chemokines [111], which can be studied in the future using the constructed model.

www.manaraa.com

REFERENCES

[1] A. Coleman-Jensen, C. Gregory, and A. Singh, "Household Food Security in the United States in 2013," *Ssrn*, no. September, 2015.

[2] E. J. Benjamin *et al.*, *Heart Disease and Stroke Statistics—2017 Update: A Report From the American Heart Association*, vol. 135, no. 10. 2017.

[3] H. K. Seligman, B. a Laraia, and M. B. Kushel, "Food Insecurity Is Associated with Chronic Disease among Low-Income," *Nutr. Dis.*, vol. 140, pp. 304–310, 2009.

[4] D. Mozaffarian, "Dietary and Policy Priorities for Cardiovascular Disease, Diabetes, and Obesity – A Comprehensive Review," *Circulation*, vol. 133, no. 2, pp. 187–225, 2017.

[5] H. Vorster and A. Kruger, "Poverty, malnutrition, underdevelopment and cardiovascular disease: a South African perspective," *Cardiovasc. J. AFRICA Cardiovasc J Afr*, vol. 18, no. 18, pp. 321–324, 2007.

[6] L. M. Klevay and G. F. Combs, "Mineral elements related to cardiovascular health," *Nutr. Drink. Water*, no. 14, pp. 92–100, 2005.

[7] R. Micha, J. L. Peñalvo, F. Cudhea, F. Imamura, C. D. Rehm, and D. Mozaffarian, "Association Between Dietary Factors and Mortality From Heart Disease, Stroke, and Type 2 Diabetes in the United States," *Jama*, vol. 317, no. 9, p. 912, 2017.

[8] D. J. Fleming, K. L. Tucker, P. F. Jacques, G. E. Dallal, P. W. F. Wilson, and R. J. Wood, "Dietary factors associated with the risk of high iron stores in the elderly Framingham Heart Study cohort," *Am. J. Clin. Nutr.*, vol. 76, no. 6, 2002.

[9] A. Skalicky, A. F. Meyers, W. G. Adams, Z. Yang, J. T. Cook, and D. A. Frank, "Child food insecurity and iron deficiency anemia in low-income infants and toddlers in the United States," *Matern. Child Health J.*, vol. 10, no. 2, pp. 177–185, 2006.

[10] V. S. Tarasuk and G. H. Beaton, "Women's dietary intakes in the context of household food insecurity," *Am. Soc. Nutr. Sci.*, vol. 129, no. 3, pp. 672–679, 1999.

[11] N. York and A. M. Schmidt, "NIH Public Access," vol. 11, no. 3, pp. 193–202, 2012.

[12] K. Park and W. J. Park, "Endothelial Dysfunction : Clinical Implications in Cardiovascular Disease and Therapeutic Approaches," pp. 1213–1225, 2015.

المنارة للاستشارات
www.manaraa.com

[13] D. Tousoulis *et al.*, "Endothelial dysfunction in conduit arteries and in microcirculation. Novel therapeutic approaches," *Pharmacol. Ther.*, vol. 144, no. 3, pp. 253–267, 2014.

[14] R. Rubinshtein *et al.*, "Assessment of endothelial function by non-invasive peripheral arterial tonometry predicts late cardiovascular adverse events," *Eur. Heart J.*, vol. 31, no. 9, pp. 1142–1148, 2010.

[15] J. E. Deanfield, J. P. Halcox, and T. J. Rabelink, "Endothelial function and dysfunction: Testing and clinical relevance," *Circulation*, vol. 115, no. 10, pp. 1285–1295, 2007.

[16] U. Förstermann and T. Münzel, "Endothelial nitric oxide synthase in vascular disease: From marvel to menace," *Circulation*, vol. 113, no. 13, pp. 1708–1714, 2006.

[17] L. J. U. Library, "eNOS Uncoupling in Cardiovascular Diseases - the Role of Oxidative Stress and Inflammation," *Ann. Vasc. Surg.*, vol. 29, no. 6, pp. 1066–1067, 2019.

[18] A. Taddei *et al.*, "Endothelial adherens junctions control tight junctions by VE-cadherin-mediated upregulation of claudin-5," *Nat. Cell Biol.*, vol. 10, no. 8, pp. 923–934, 2008.

[19] P. K. Mehta and K. K. Griendling, "Angiotensin II cell signaling: physiological and pathological effects in the cardiovascular system," *Am. J. Physiol. - Cell Physiol.*, vol. 292, no. 1, pp. C82–C97, 2007.

[20] Y. Taniyama and K. K. Griendling, "Reactive Oxygen Species in the Vasculature: Molecular and Cellular Mechanisms," *Hypertension*, vol. 42, no. 6, pp. 1075–1081, 2003.

[21] R. M. Touyz, "Reactive oxygen species and angiotensin II signaling in vascular cells - Implications in cardiovascular disease," *Brazilian J. Med. Biol. Res.*, vol. 37, no. 8, pp. 1263–1273, 2004.

[22] X.-L. Chen, "Activation of Nrf2/ARE pathway protects endothelial cells from oxidant injury and inhibits inflammatory gene expression," *AJP Hear. Circ. Physiol.*, vol. 290, no. 5, pp. H1862–H1870, 2006.

[23] C. Sen and L. Packer, "Antioxidant and redox regulation of gene transcription," *Faseb*, vol. 10, no. 7, pp. 709–720, 1996.

[24] S. Wu *et al.*, "Activation of AP-1 through reactive oxygen species by angiotensin II in rat cardiomyocytes," *Free Radic. Biol. Med.*, vol. 39, no. 12, pp. 1601–1610, 2005.

[25] M. Ushio-Fukai, A. Maziar Zafari, T. Fukui, N. Ishizaka, and K. K. Griendling, "p22(phox) is a critical component of the superoxide-generating NADH/NADPH oxidase system and regulates angiotensin II-induced hypertrophy in vascular smooth muscle cells," *J. Biol. Chem.*, vol. 271, no. 38, pp. 23317–23321, 1996.

www.manaraa.com

[26] S. Rajagopalan *et al.*, "Angiotensin II–mediated Hypertension in the Rat Increases Vascular Superoxide Production via Membrane NADH/NADPH Oxidase Activation Contribution to Alterations of Vasomotor Tone," *J. Clin. Invest.*, vol. 97, no. 8, pp. 1916–1923, 1996.

[27] A. M. Zafari *et al.*, "Role of NADH/NADPH oxidase-derived H2O2in angiotensin II-induced vascular hypertrophy," *Hypertension*, vol. 32, no. 3, pp. 488–495, 1998.

[28] C. Yan, D. Kim, T. Aizawa, and B. C. Berk, "Functional interplay between Angiotensin II and nitric oxide: Cyclic GMP as a key mediator," *Arterioscler. Thromb. Vasc. Biol.*, vol. 23, no. 1, pp. 26–36, 2003.

[29] V. J. Dzau and V. J. Dzau, "Tissue Angiotensin and Pathobiology of Vascular Disease: A Unifying Hypothesis," pp. 1047–1052, 2001.

[30] G. M. Rubanyi and P. M. Vanhoutte, "Superoxide anions and hyperoxia inactivate endothelium-derived relaxing factor," *Am. J. Physiol. Circ. Physiol.*, vol. 250, no. 5, pp. H822–H827, 1986.

[31] M. A. Reidy and S. M. Schwartz, "A technique to investigate surface morphology and endothelial cell replication of small arteries: A study in acute angiotensin-induced hypertensive rats," *Microvasc. Res.*, vol. 24, no. 2, pp. 158–167, 1982.

[32] Y. Shen *et al.*, "Granzyme B De fi ciency Protects against Angiotensin II e Induced Cardiac Fibrosis," vol. 186, no. 1, 2016.

[33] I. A. Ikhapoh, C. J. Pelham, and D. K. Agrawal, "Synergistic effect of angiotensin II on vascular endothelial growth factor-A-mediated differentiation of bone marrow-derived mesenchymal stem cells into endothelial cells," *Stem Cells Int.*, vol. 2015, pp. 1–13, 2015.

[34] N. Rudini *et al.*, "VE-cadherin is a critical endothelial regulator of TGF-β signalling," *EMBO J.*, vol. 27, no. 7, pp. 993–1004, 2008.

[35] J. A. Ardura, S. Rayego-Mateos, D. Ramila, M. Ruiz-Ortega, and P. Esbrit, "Parathyroid Hormone-Related Protein Promotes Epithelial-Mesenchymal Transition," *J. Am. Soc. Nephrol.*, vol. 21, no. 2, pp. 237–248, 2010.

[36] Y. C. Tian and A. O. Phillips, "Interaction between the Transforming Growth Factor-β Type II Receptor/Smad Pathway and β-Catenin during Transforming Growth Factor-β1-Mediated Adherens Junction Disassembly," *Am. J. Pathol.*, vol. 160, no. 5, pp. 1619–1628, 2002.

[37] T. Neunteufl, S. Heher, T. Stefenelli, I. Pabinger, and H. Gisslinger, "Endothelial dysfunction in patients with polycythaemia vera," *Br. J. Haematol.*, vol. 115, no. 2, pp. 354–359, 2001.

www.manaraa.com

[38] L. V Beerepoot, D. T. Shi, K. Yeo, and E. E. Voest, "Up-Regulation of Vascular Endothelial Growth Factor Production by Iron Chelators," vol. 1, pp. 3747–3752, 1996.

[39] Y. Yang, Y. Xu, A. Su, D. Yang, and X. Zhang, "Effects of Deferoxamine on Leukemia In Vitro and Its Related Mechanism," *Med. Sci. Monit.*, vol. 24, pp. 6735–6741, 2018.

[40] S. Tajima *et al.*, "Iron reduction by deferoxamine leads to amelioration of adiposity via the regulation of oxidative stress and inflammation in obese and type 2 diabetes KKAy mice," *Am. J. Physiol. Metab.*, vol. 302, no. 1, pp. E77–E86, 2011.

[41] M. D. Knutson, P. B. Walter, B. N. Ames, and F. E. Viteri, "Both Iron Deficiency and Daily Iron Supplements Increase Lipid Peroxidation in Rats," *J. Nutr.*, vol. 130, no. 3, pp. 621–628, 2000.

[42] M. K. Shigenaga, T. M. Hagen, and B. N. Ames, "Oxidative damage and mitochondrial decay in aging.," *Proc. Natl. Acad. Sci.*, vol. 91, no. 23, pp. 10771–10778, 1994.

[43] P. B. Walter *et al.*, "Iron deficiency and iron excess damage mitochondria and mitochondrial DNA in rats," 2001.

[44] C. Biology, "Mitochondrial Diseases in Man and Mouse," *Science (80-.).*, vol. 1482, no. 1999, pp. 1482–1489, 2009.

[45] D. Y. Li, Y. C. Zhang, M. I. Philips, T. Sawamura, and J. L. Mehta, "Upregulation of endothelial receptor for oxidized low-density lipoprotein (LOX-1) in cultured human coronary artery endothelial cells by angiotensin II type 1 receptor activation," *Circ.Res.*, vol. 84, no. 9, pp. 1043–1049, 1999.

[46] A. W. Feinberg *et al.*, "Controlling the contractile strength of engineered cardiac muscle by hierarchal tissue architecture," *Biomaterials*, vol. 33, no. 23, pp. 5732–5741, 2012.

[47] J. S. Sham, S. N. Hatem, and M. Morad, "Species differences in the activity of the Na(+)???Ca2+ exchanger in mammalian cardiac myocytes.," *J. Physiol.*, vol. 488, no. 3, pp. 623–631, 1995.

[48] A. Zaupa, "Physical crosslinking of gelatin: A supramolecular approach to biomaterials," p. 167, 2010.

[49] A. Bettadapur *et al.*, "Prolonged Culture of Aligned Skeletal Myotubes on Micromolded Gelatin Hydrogels," *Nat. Publ. Gr.*, pp. 1–14, 2016.

[50] M. L. McCain, A. Agarwal, H. W. Nesmith, A. P. Nesmith, and K. K. Parker, "Micromolded gelatin hydrogels for extended culture of engineered cardiac tissues," *Biomaterials*, vol. 35, no. 21, pp. 5462–5471, 2014.

[51] A. Paguirigan and D. J. Beebe, "Gelatin based microfluidic devices for cell culture," *Lab Chip*, vol. 6, no. 3, pp. 407–413, 2006.

www.manaraa.com

[52] D. Y. S. Chau, R. J. Collighan, E. A. M. Verderio, V. L. Addy, and M. Griffin, "The cellular response to transglutaminase-cross-linked collagen," *Biomaterials*, vol. 26, no. 33, pp. 6518–6529, 2005.

[53] D. E. Discher, P. Janmey, and Y. L. Wang, "Tissue cells feel and respond to the stiffness of their substrate," *Science (80-.).*, vol. 310, no. 5751, pp. 1139–1143, 2005.

[54] B. N. Mason, A. Starchenko, R. M. Williams, L. J. Bonassar, and C. A. Reinhart-King, "Tuning three-dimensional collagen matrix stiffness independently of collagen concentration modulates endothelial cell behavior," *Acta Biomater.*, vol. 9, no. 1, pp. 4635–4644, 2013.

[55] R. G. Wells, "The role of matrix stiffness in regulating cell behavior," *Hepatology*, vol. 47, no. 4, pp. 1394–1400, 2008.

[56] T. Yeung *et al.*, "Effects of substrate stiffness on cell morphology, cytoskeletal structure, and adhesion," *Cell Motil. Cytoskeleton*, vol. 60, no. 1, pp. 24–34, 2005.

[57] F. J. Byfield, R. K. Reen, T. P. Shentu, I. Levitan, and K. J. Gooch, "Endothelial actin and cell stiffness is modulated by substrate stiffness in 2D and 3D," *J. Biomech.*, vol. 42, no. 8, pp. 1114–1119, 2009.

[58] A. L. Sieminski, R. P. Hebbel, and K. J. Gooch, "The relative magnitudes of endothelial force generation and matrix stiffness modulate capillary morphogenesis in vitro," *Exp. Cell Res.*, vol. 297, no. 2, pp. 574–584, 2004.

[59] J. A. Wood *et al.*, "The role of substratum compliance of hydrogels on vascular endothelial cell behavior," *Biomaterials*, vol. 32, no. 22, pp. 5056–5064, 2011.

[60] L. Davenport Huyer *et al.*, "Highly Elastic and Moldable Polyester Biomaterial for Cardiac Tissue Engineering Applications," *ACS Biomater. Sci. Eng.*, vol. 2, no. 5, pp. 780–788, 2016.

[61] A. M. Nair *et al.*, "The effect of erythropoietin on autologous stem cell-mediated bone regeneration," *Biomaterials*, vol. 34, no. 30, pp. 7364–7371, 2013.

[62] S. L. Pereira *et al.*, "Inhibition of mitochondrial complex III blocks neuronal differentiation and maintains embryonic stem cell pluripotency," *PLoS One*, vol. 8, no. 12, pp. 1–16, 2013.

[63] Z. X. Liao, Y. C. Li, H. M. Lu, and H. W. Sung, "A genetically-encoded KillerRed protein as an intrinsically generated photosensitizer for photodynamic therapy," *Biomaterials*, vol. 35, no. 1, pp. 500–508, 2014.

[64] A. Bender *et al.*, "TOM40 Mediates Mitochondrial Dysfunction Induced by α-Synuclein Accumulation in Parkinson's Disease," *PLoS One*, vol. 8, no. 4, 2013.

www.manaraa.com

[65] R. B. Hamanaka and N. S. Chandel, “Mitochondrial reactive oxygen species regulate cellular signaling and dictate biological outcomes,” *Trends Biochem. Sci.*, vol. 35, no. 9, pp. 505–513, 2010.

[66] K. Saha *et al.*, “Substrate modulus directs neural stem cell behavior.,” *Biophys. J.*, vol. 95, no. 9, pp. 4426–38, 2008.

[67] E. N. Haugen, A. J. Croatt, and K. A. Nath, “Angiotensin ii induces renal oxidant stress in vivo and heme oxygenase-1 in vivo and in vitro,” *Kidney Int.*, vol. 58, no. 1, pp. 144–152, 2000.

[68] P. RE:, “Angiotensin II and the control of cardiovascular structure.,” *J Am Soc Nephrol*, vol. 30, no. 3. pp. 364–367, 1999.

[69] K. K. Griendling, C. A. Minieri, J. D. Ollerenshaw, and R. W. Alexander, “Angiotensin II Stimulates NADH and NADPH Oxidase Activity in Cultured Vascular Smooth Muscle Cells Key Words * NADH oxidase * NADPH oxidase vascular smooth muscle * angiotensin II * superoxide anion A,” *Circ Res*, vol. 74, pp. 1141–1148, 1994.

[70] E. A. Jaimes, J. M. Galceran, and L. Raij, “Angiotensin II induces superoxide anion production by mesangial cells,” *Kidney Int.*, vol. 54, no. 3, pp. 775–784, 1998.

[71] T. Hannken, R. Schroeder, R. A. K. Stahl, and G. Wolf, “Angiotensin II-mediated expression of p27Kip1 and induction of cellular hypertrophy in renal tubular cells depend on the generation of oxygen radicals[1]1See Editorial by Shankland, p. 2241.,” *Kidney Int.*, vol. 54, no. 6, pp. 1923–1933, 2002.

[72] S. Klahr and J. Morrissey, “Angiotensin II and gene expression in the kidney,” *Am. J. Kidney Dis.*, vol. 31, no. 1, pp. 171–176, 1998.

[73] X. Yuan *et al.*, “Regulation of LIP level and ROS formation through interaction of H-ferritin with G-CSF receptor,” *J. Mol. Biol.*, vol. 339, no. 1, pp. 131–144, 2004.

[74] N. C. Andrews, “Disorders of Iron Metabolism,” *N. Engl. J. Med.*, vol. 341, no. 26, pp. 1986–1995, 1999.

[75] J. R. and V. JAGADEESAN, “LIPID PEROXIDATION AND ACTIVITIES OF ANTIOXIDANT ENZYMES IN IRON DEFICIENCY AND EFFECT OF CARCINOGEN FEEDING,” vol. 21, no. 1, pp. 103–108, 1996.

[76] Y. Mikhed, A. Daiber, and S. Steven, “Mitochondrial oxidative stress, mitochondrial DNA damage and their role in age-related vascular dysfunction,” *Int. J. Mol. Sci.*, vol. 16, no. 7, pp. 15918–15953, 2015.

[77] O. Htm and W. H. Ratzburg, “Iron Starvation Leads to Oxidative Stress in Anabaena sp. Strain PCC 7120,” vol. 187, no. 18, pp. 1–6, 2001.

www.manaraa.com

[78] SCHLONDORFF and D., "The role of chemokines in the initiation and progression of renal disease," *Kidney Int*, vol. 47, no. 49, pp. S44–S47, 1995.

[79] E. Haugen and K. A. Nath, "The Involvement of Oxidative Stress in the Progression of Renal Injury," vol. 55905, pp. 58–65, 1999.

[80] J. J. P. and J. E. Oscar Lorenzo and M. A. H.-P. Marta Ruiz-Ortega, Carmen Bustos, "Angiotensin II participates in mononuclear cell recruitment in experimental immune complex Nephritis Through Nuclear Factor-κB Activation Synthesis and Monocyte Chemoattractant Protein-1." .

[81] S. Kagami, W. A. Border, D. E. Miller, and N. A. Noble, "Angiotensin II stimulates extracellular matrix protein synthesis through induction of transforming growth factor-β expression in rat glomerular mesangial cells," *J. Clin. Invest.*, vol. 93, no. 6, pp. 2431–2437, 1994.

[82] G. Wolf *et al.*, "Angiotensin II stimulates expression of the chemokine RANTES in rat glomerular endothelial cells. Role of the angiotensin type 2 receptor," *J. Clin. Invest.*, vol. 100, no. 5, pp. 1047–1058, 1997.

[83] K. Yoshioka *et al.*, "Endothelial PI3K-C2α, a class II PI3K, has an essential role in angiogenesis and vascular barrier function," *Nature Medicine*, vol. 18, no. 10. pp. 1560–1569, 2012.

[84] C. Pupilli *et al.*, "Angiotensin II Stimulates the Synthesis and Secretion of Vascular Permeability Factor/Vascular Endothelial Growth Factor in Human Mesangial Cells," no. 12, pp. 245–255, 1999.

[85] H. Sano, K. Hosokawa, H. Kidoya, and N. Takakura, "Negative regulation of VEGF-induced vascular leakage by blockade of angiotensin II type 1 receptor," *Arterioscler. Thromb. Vasc. Biol.*, vol. 26, no. 12, pp. 2673–2680, 2006.

[86] W. G. G. Roberts and G. E. G. E. Palade, "Increased microvascular permeability and endothelial fenestration induced by vascular endothelial growth factor.," *J. Cell Sci.*, vol. 108 (Pt 6, no. 6, pp. 2369–79, 1995.

[87] J. Gavard and J. S. Gutkind, "VEGF Controls endothelial-cell permeability promoting β-arrestin-dependent Endocytosis VE-cadherin," *Nat. Cell Biol.*, vol. 8, no. 11, pp. 1223–1234, 2006.

[88] A. Broermann *et al.*, "Dissociation of VE-PTP from VE-cadherin is required for leukocyte extravasation and for VEGF-induced vascular permeability in vivo," *J. Exp. Med.*, vol. 208, no. 12, pp. 2393–2401, 2011.

[89] S. Esser, M. G. Lampugnani, M. Corada, E. Dejana, and W. Risau, "Vascular endothelial growth factor induces VE-cadherin tyrosine phosphorylation in endothelial cells.," *J. Cell Sci.*, vol. 111 (Pt 1, pp. 1853–65, 1998.

www.manaraa.com

[90] F. H. and J. Huot, “Dysregulation of the Endothelial CellularResponse to Oxidative Stress in Cancer,” *Mol. Carcinog.*, vol. 329, no. August 2006, pp. 315–329, 2007.

[91] P. L. Apopa *et al.*, “Iron oxide nanoparticles induce human microvascular endothelial cell permeability through reactive oxygen species production and microtubule remodeling,” *Part. Fibre Toxicol.*, vol. 6, pp. 1–14, 2009.

[92] T. N. Meyer, C. Schwesinger, J. Ye, B. M. Denker, and S. K. Nigam, “Reassembly of the Tight Junction after Oxidative Stress Depends on Tyrosine Kinase Activity,” *J. Biol. Chem.*, vol. 276, no. 25, pp. 22048–22055, 2001.

[93] and G. W. H. D. Michael Shasby, Stuart E. Lind, Sandra S. Shasby, Jonathan C. Goldsmith, “Reversible Oxidant-Induced Increases in Albumin Transfer Across Cultured Endothelium: Alterations in Cell Shape and Calcium Homeostasis,” vol. 74, no. 4, pp. 1424–1427, 2018.

[94] A. Hashimoto-Komatsu, T. Hirase, M. Asaka, and K. Node, “Angiotensin II induces microtubule reorganization mediated by a deacetylase SIRT2 in endothelial cells,” *Hypertens. Res.*, vol. 34, no. 8, pp. 949–956, 2011.

[95] J. P. M. Wesselman and J. G. R. De Mey, “Angiotensin and cytoskeletal proteins: Role in vascular remodeling,” *Curr. Hypertens. Rep.*, vol. 4, no. 1, pp. 63–70, 2002.

[96] E. M. de Cavanagh, M. Ferder, F. Inserra, and L. Ferder, “Angiotensin II, mitochondria, cytoskeletal, and extracellular matrix connections: an integrating viewpoint,” *Am. J. Physiol. Circ. Physiol.*, vol. 296, no. 3, pp. H550–H558, 2009.

[97] F. Dong, X. Zhang, B. Culver, H. G. Chew, R. O. Kelley, and J. Ren, “Dietary iron deficiency induces ventricular dilation , mitochondrial ultrastructural aberrations and cytochrome c release : involvement of nitric oxide synthase and protein tyrosine nitration,” vol. 286, pp. 277–286, 2005.

[98] A. Swali, S. McMullen, H. Hayes, L. Gambling, H. J. McArdle, and S. C. Langley-Evans, “Cell cycle regulation and cytoskeletal remodelling are critical processes in the nutritional programming of embryonic development,” *PLoS One*, vol. 6, no. 8, pp. 1–10, 2011.

[99] K. E. Brunette, P. V. Tran, J. D. Wobken, E. S. Carlson, and M. K. Georgieff, “Gestational and neonatal iron deficiency alters apical dendrite structure of CA1 pyramidal neurons in adult rat hippocampus,” *Dev. Neurosci.*, vol. 32, no. 3, pp. 238–248, 2010.

[100] J. S. Y. Lee and A. I. Gotlieb, “Microtubule-actin interactions may regulate endothelial integrity and repair,” *Cardiovasc. Pathol.*, vol. 11, no. 3, pp. 135–140, 2002.

[101] J. Behrens, “Cadherins and catenins: Role in signal transduction and tumor progression,” *Cancer Metastasis Rev.*, vol. 18, no. 1, pp. 15–30, 1999.

www.manaraa.com

[102] M. A. Gimbrone and and G. García-Cardeña, “Vascular endothelium, hemodynamics, and the pathobiology of atherosclerosis,” vol. 22, no. 1, pp. 9–15, 2015.

[103] J. N. Topper and M. A. Gimbrone, “Blood flow and vascular gene expression: Fluid shear stress as a modulator of endothelial phenotype,” *Mol. Med. Today*, vol. 5, no. 1, pp. 40–46, 1999.

[104] K.-R. Q. Zong-Zheng Chen, Wei-MO Yuan, Cheng Xiang, De-pi Zeng, Bo Liu, “A microfludic device with spatiotemporal wall shear atress and ATP signals to investigate the intracellular calcium dynamics in vascular endothelial cells.” p. 14, 2018.

[105] C. Camello-Almaraz, P. J. Gomez-Pinilla, M. J. Pozo, and P. J. Camello, “Mitochondrial reactive oxygen species and Ca2+ signaling,” *Am. J. Physiol. - Cell Physiol.*, vol. 291, no. 5, pp. 1082–1088, 2006.

[106] C. Tiruppathi, R. D. Minshall, B. C. Paria, S. M. Vogel, and A. B. Malik, “Role of Ca2+ signaling in the regulation of endothelial permeability,” *Vascul. Pharmacol.*, vol. 39, no. 4–5, pp. 173–185, 2002.

[107] J. Seebach *et al.*, “Endothelial Barrier Function under Laminar Fluid Shear Stress,” vol. 80, no. 12, pp. 1819–1831, 2000.

[108] J. P. Navas *et al.*, “Regulation of endothelial cell nitric oxide synthase mRNA expression by shear stress,” 2019.

[109] T. Bachetti and L. Morbidelli, “Endothelial cells in culture: A model for studying vascular functions,” *Pharmacol. Res.*, vol. 42, no. 1, pp. 9–19, 2000.

[110] B. G. Chung, K. Lee, and S. Lee, “Lab on a Chip Microfluidic fabrication of microengineered hydrogels and their application in,” pp. 45–59, 2012.

[111] J. P. J. Halcox, “Endothelial Dysfunction,” *Prim. Auton. Nerv. Syst.*, no. 12, pp. 319–324, 2012.

[112] Shah SV: The role of reactive oxygen metabolites in glomerular disease. Annu Rev Physiol 57:245–262, 1995.

[113] Holman RG, Maier RV: Oxidant-induced endothelial leak correlates with decreased cellular energy levels. Am Rev Respir Dis 1990, 141(1):134-140.

[114] Remuzzi A, Dewey CF Jr, Davies PF, Gimbrone MA Jr. “Orientation of endothelial cells in shear fields in vitro.,” vol.21, Biorheology. 1984;21(4):617-30.

www.manaraa.com

APPENDIX A

SUPPLEMENTARY FIGURES FOR KINETIC OXIDATIVE STRESS ASSAY

www.manaraa.com

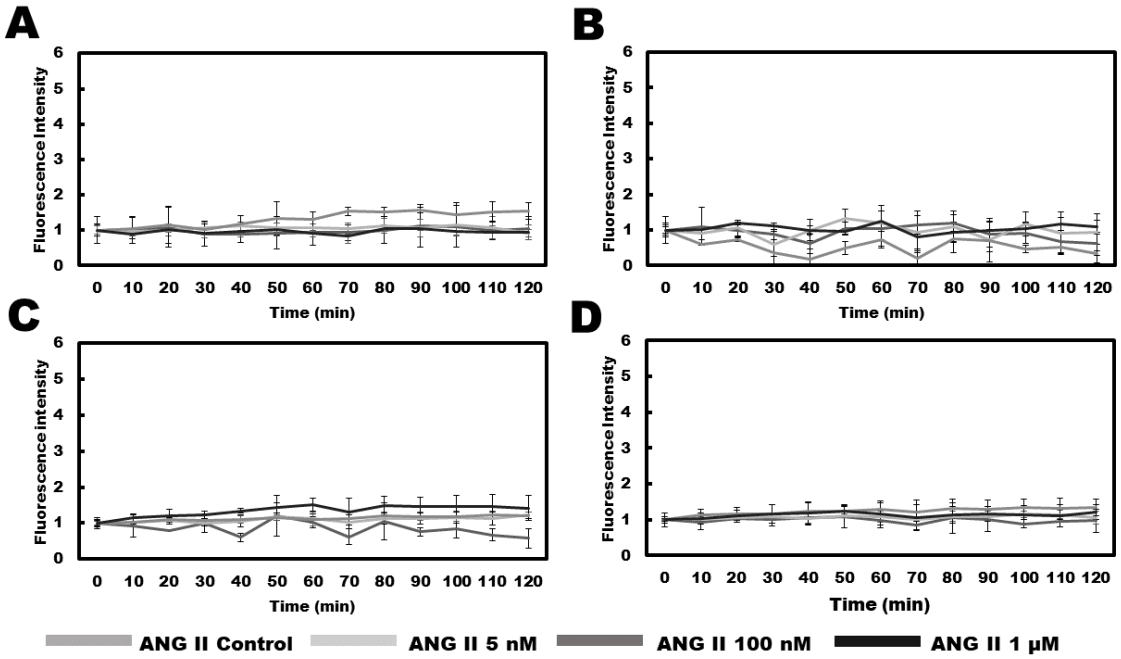

Figure A.1 Angiotensin II induced kinetic ROS production.

The kinetic study was done for 2 hours in every 10 minutes. (A) The graph represents the kinetic reactive oxygen species production by HCMVEC treated with 0, 5 nM, 100 nM, 1 µM ANG II for 1 hour. (B) The graph represents the kinetic reactive oxygen species production by HCMVEC treated with 0, 5 nM, 100 nM, 1 µM ANG II for 24 hours. (C) The graph represents the kinetic reactive oxygen species production by HCMVEC treated with 0, 5 nM, 100 nM, 1 µM ANG II for 72 hours. (D) The graph represents the kinetic reactive oxygen species production by HCMVEC treated with 0, 5 nM, 100 nM, 1 µM ANG II for 1 week. (n=3, Mean ± Standard deviation)

www.manaraa.com

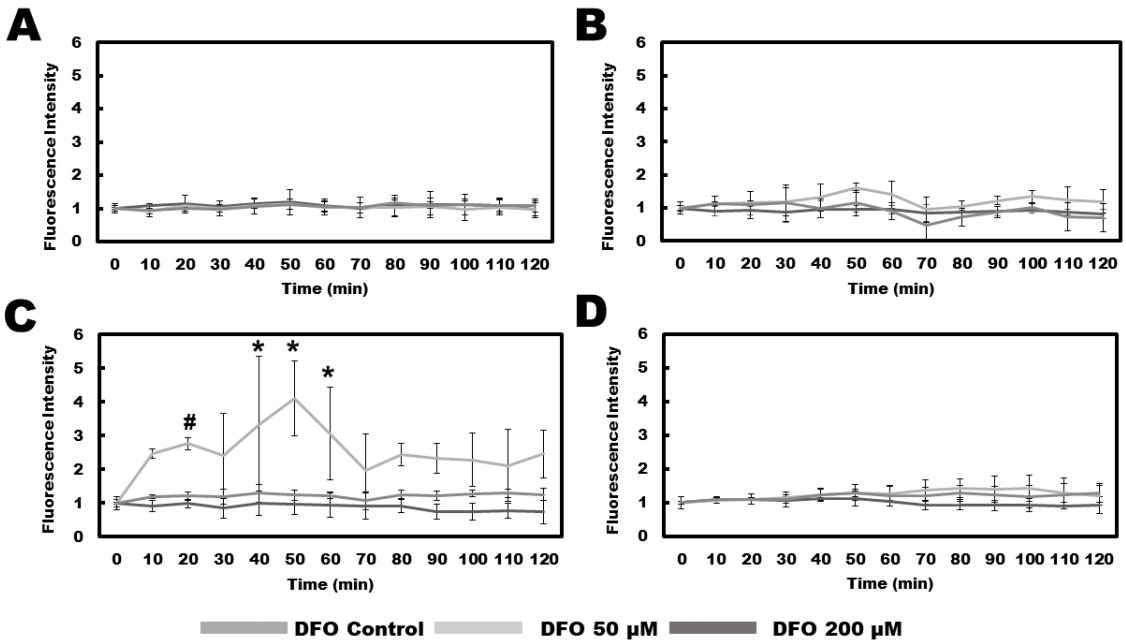

Figure A.2 Deferoxamine induced kinetic ROS production.

The kinetic study was done for 2 hours in every 10 minutes. (A) The graph represents the kinetic reactive oxygen species production by HCMVEC treated with 0, 50 µM, 200 µM DFO for 1 hour. (B) The graph represents the kinetic reactive oxygen species production by HCMVEC treated with 0, 50 µM, 200 µM DFO for 24 hours. (C) The graph represents the kinetic reactive oxygen species production by HCMVEC treated with 0, 50 µM, 200 µM DFO for 72 hours. (D) The graph represents the kinetic reactive oxygen species production by HCMVEC treated with 0, 50 µM, 200 µM DFO for 1 week. (n=3, Mean ± Standard deviation, * indicates P-value < 0.01 relative to 0 minute and # indicates P-value < 0.05 relative to 0 minute)

www.manaraa.com